UNIVERSITAT POLITÈCNICA DE CATALUNYA
BARCELONATECH
Escola d'Enginyeria de Barcelona Est

FINAL PROJECT

Mechanical Engineering

STUDY OF MECHANICAL PROPERTIES OF SPECIMENS MANUFACTURED BY FFF

Author: Marc Mimbrero Gallardo
Director: Jose Antonio Travieso Rodríguez
Location: Escola d'Enginyeria de Barcelona Est (EEBE)

Call: April 2019

Resum

El present projecte té com a finalitat l'estudi de les propietats mecàniques del Timberfill segons els paràmetres de fabricació utilitzats, analitzant-les en assajos a flexió a quatre punts. Per l'estudi s'utilitzarà com a mètode de fabricació de provetes el FDM (Fused Deposition Material).

Per realitzar l'estudi es variaran els següents paràmetres a l'hora d'imprimir les provetes: alçada de capa, velocitat d'impressió, diàmetre de l'extrusor i la densitat d'emplenament. Es mantindran constants l'estructura d'emplenament, que serà del tipus Honeycomb, i l'orientació d'impressió, realitzada sobre l'eix "X".

Les dimensions de les provetes i l'assaig es duran a terme segons la normativa ASTM D6272. Per optimitzar el projecte, s'utilitzarà un disseny d'experiments tipus Taguchi per reduir el nombre de provetes impreses i assajades.

Un cop impreses, s'estudiaran a flexió a quatre punts. El test es realitzarà aplicant la mateixa càrrega de força a totes les mostres i la proveta que presenti un major radi de flexió, sense trencament, serà la combinació òptima.

S'analitzaran els resultats mitjançant l'anàlisi ANOVA (Analisys of Variance). Amb aquest anàlisi es determinarà la influència dels paràmetres d'impressió sobre les propietats mecàniques del Timberfill.

Finalment, es conclourà quina és la combinació de paràmetres d'impressió òptims i la influència de cadascun, dintre del rang de paràmetres analitzat.

Resumen

El presente proyecto tiene como finalidad el estudio de las propiedades mecánicas del Timberfill según los parámetros de fabricación utilizados, analizadas en ensayos a flexión a cuatro puntos. Para el estudio se utilizará como método de fabricación de probetas FDM (Fused Deposition Material).

Para realizar el estudio se variarán los siguientes parámetros a la hora de imprimir las probetas: altura de capa, velocidad de impresión, diámetro del extrusor y la densidad de llenado. Se mantendrán constantes el patrón de llenado, que será del tipo Honeycomb, y la orientación de impresión, realizada sobre el eje "X".

Las dimensiones de las probetas y el ensayo se llevarán a cabo según la normativa ASTM D6272. Para optimizar el proyecto, se utilizará un diseño de experimentos tipo de Taguchi para reducir el número de probetas impresas y ensayadas.

Unavez imprimidas, se estudiarán a flexión a cuatro puntos. El test se realizará aplicando la misma carga de fuerza a todas las muestras y la probeta que presente un mayor radio de flexión, sin rotura, será la combinación óptima.

Se analizarán los resultados mediante el análisis ANOVA (Analisys of Variance). Con este análisis se determinará la influencia de los parámetros de impresión sobre las propiedades mecánicas del Timberfill.

Finalmente, se concluirá cuál es la combinación de parámetros de impresión óptimos y la influencia de cada uno, dentro del rango de parámetros analizado.

Abstract

This project aims to study the mechanical properties of Timberfill of parts manufactured using FFF (Fused Filament Fabrication) technology. For this study, the influences of four parameters on flexural property (four point bending) of Timberfill parts are considered.

During this process, the following parameters are varied in three different levels: layer height, printing speed, nozzle diameter, and fill density. All of the samples are printed with honeycomb infill pattern and the printing orientation on "0-X" axis.

The specific shape and geometry of the samples and the test configuration are performed according to the ASTM D6272 standard. An experimental design Taguchi method is performed to optimize the project and avoid to make a large numbers of specimens.

The tests carried out by applying the same load to all of the samples.

The results are analyzed through analyze of variance (ANOVA) to determine the influence of the manufacturing parameters mechanical properties of Timberfill material.

Finally, it concluded which is the optimal combination of printing parameters and the influence of each one, within the analyzed ratio of parameters.

Acknowledgements

I would like to thank the people who has been involved in this project and helped me to carry it out.

Specially, I would like to thank to M. Damous Zandi for all the time dedicated on this project and in personal aspect. It has been a pleasure work hand by hand with him during the whole year that this project past, due to his useful suggestions, ideas and technical knowledge.

I would also like to thank to J. Llumà, for the technical support given, and to J.A. Travieso to agree be the director of my project and supervise it.

Finally, I would like to thank to my family and friends for the motivation to carry on the project.

Index of figure

Figure 1: Overview of the FFF printer [5]
Figure 2: Clarifying layer height [8]
Figure 3: Infill patterns [11]
Figure 4: Infill percentages 25%, 50%, 75%. [12]
Figure 5: Different printing orientation [13]
Figure 6: Timberfill champagne spool [21]
Figure 7: Technical data sheet developed by manufacturer [21]
Figure 8: Linear graph of orthogonal arra [22]y
Figure 9: Dimensions of test specimens: 80 x 10 x 4 mm, [23]
Figure 10: Pyramid studio 3D printer [6]
Figure 11: Plan of the cross section [6]
Figure 12: Different infill shape of 5 samples
Figure 13: Primary and solid bottom and top determined layers
Figure 14: Specimens printed with 25%, 50%, 70% infill density and the sample on the printer's bed
Figure 15: Template of metrology. Source: DEFAM
Figure 16: Universal material testing machine, zwick roell Z020 [22]
Figure 17: Loading diagram [23]
Figure 18: Loading Noses and Supports (Example of One Third of support span) [23]
Figure 19: Block diagram of the equipment [22]
Figure 20: Camera assembly [22]
Figure 21: Initial position
Figure 22: Drawing of the synchronize [6]
Figure 23: Generated grids
Figure 24: Image processing
Figure 25: calculating Pixel/mm ratio
Figure 26: Excel calculation sheet
Figure 27: Main effect of means on Young modulus
Figure 28: Interaction plot of means on Young modulus
Figure 29: Main plot for S/N ratio, Young modulus
Figure 30: Residual plot for means, Young's modulus
Figure 31: Main effect of means on Elastic limit
Figure 32: Interaction plot of means on Elastic limit
Figure 33: Main plot for S/N ratio, Elastic limit
Figure 34: Residual plot for means, Elastic limit
Figure 35: Main effects plot for means, Maximum tension
Figure 36: Interaction plot for means, Maximum tension
Figure 37: Main effect plot for S/N ratio, Maximum tension
Figure 38: Residual plot for means, Maximum tension
Figure 39: Main effects plot for means, Maximum elongation

Figure 40: Interaction plot for means, Maximum elongation
Figure 41: Main effect plot for S/N ratio, Maximum elongation
Figure 42: Residual plot for means, Maximum elongation

Index of table

Table 1: Factors and levels used for the DOE.
Table 2: L27 Taguchi orthogonal array for the DOE
Table 3: Table of results
Table 4: p-values of means, Young modulus
Table 5: p-value interaction of means, Young modulus
Table 6: p-values of S/N ratio, Young modulus
Table 7: p-values of means, Elastic limit
Table 8: p-value interaction of means, Elastic limit
Table 9: p-values of S/N ratio, Elastic limit
Table 10: p-values of means, Maximum tension
Table 11: p-value interaction of means, Maximum tension
Table 12: p-values of S/N, Maximum tension
Table 13: p-values of means, Maximum elongation
Table 14: p-value interaction of means, Maximum elongation
Table 15: p-values of S/N, Maximum elongation
Table 16: Abstract of results and significance
Table 17: Optimized level of parameters
Table 18: PLA levels of best combination
Table 19: Maximum values achieved for PLA/Timberfill
Table 20: Cost of Timberfill
Table 21: Consumible equipment
Table 22: Energy cost
Table 23: Human resources cost
Table 24: Summary cost

Index

RESUM I

RESUMEN II

ABSTRACT III

ACKNOWLEDGEMENTS V

INDEX OF FIGURE VII

INDEX OF TABLE IX

1. INTRODUCTION 1

1.1. Objectives 1

1.2. Motivation 2

2. STATE OF ART 3

2.1. Additive manufacturing methods 3

2.2. FFF technology 4

2.2.1. Layer height 5

2.2.2. Nozzle diameter 5

2.2.3. Infill pattern 5

2.2.4. Fill density 6

2.2.5. Printing velocity 7

2.2.6. Printing orientation 7

2.3. Materials 8

2.4. Mechanical properties 9

3. MANUFACTURING DESIGN 10

3.1. Specimen fabrication 13

3.2. Metrology 16

3.3. Test machine and procedure 17

3.4. Experimental setup 21

4. ANALYZING PROCESS 23

5. RESULTS 27

6. RESULTS ANALYSIS 28

6.1. Young modulus 28
6.2. Elastic limit ($Rp_{0.2}$) 33
6.3. Maximum tension (σ_{max}) 36
6.4. Maximum elongation 40

7. RESULTS DISCUSSION 44
7.1. Layer height 45
7.2. Nozzle diameter 45
7.3. Infill density 45
7.4. Printing velocity 46

8. COMPARISON BETWEEN PLA/TIMBERFILL 47

9. CONCLUSION 49

BUDGET 51

BIBLIOGRAPHY 57

1. Introduction

1.1. Objectives

The main purpose of this project is to study the mechanical properties of a relatively new material such as Timberfill. In order to complete the project, the samples will be printed using the technique of additive manufacturing and will be analysed to four point bending test, following the methodology of other works [6, 22].

The procedure will be:

- Manufacture the specimens using a 3D printer, following established parameters which vary depending on the sample, and according to the standard ASTM D6272. An L27 Taguchi orthogonal array is selected to conduct the experimental phase.
- Apply four point bending test method for Timberfill material.
- Using analyse of variance (ANOVA) to achieve the optimal combination of parameters and selected levels.
- Compare the obtained results for this material with other common used such as PLA

1.2. Motivation

Capability of 3D printing technology is growing further in engineering and industrial fields due to its advantages: using less material than another manufacturing technics such as casting, laser, etc. It also allows to obtain pieces in a faster way, therefore it does not require any prior process. On the other hand, its advancement to allow to manufacture pieces with a high level of details and increasing mechanical performance.

The appearance of printed parts is one of the main characteristics of Timberfill. It seems resemble to natural wood, which makes it as an interesting material for various applications.

The Timberfill is a composite material of poly lactic acid (PLA) and wood fibres. In spite of that PLA has been studied and characterized mostly, the mechanical characteristics of Timberfill are not completely considered.

Compare the mechanical properties of Timberfill with the PLA can be interesting to obtain conclusions in order to select a material in industrial uses.

All of the statements mentioned above are good reasons to study the characteristics of Timberfill.

2. State of art

One of the most common processes of additive manufacturing is 3D printing. It appeared in the 80's and over the years has become more significant. Since 1990's to the time being is rising continuously to obtain pieces with more details and better mechanical properties, as well as the appearance of new elements such as the Timberfill. 3D printing is considered a new industrial revolution [1] .

It began as a technology used mainly in fields like engineering and architecture, to perform prototypes of low mechanical quality and with small scale details of finish. Nowadays, been using in other fields, such as biotechnology or aerospace technology, as it has advanced so much even to print alive cells [2].

3D printing is a technology for making objects layer upon layer. To perform the pieces, first CAD (Computer-Aid Design) software is used, with which the piece is designed and its possible mechanical behavior is analyzed. Once the piece is designed, it is transferred to software that converts the piece of the CAD design and controls the printer to make the impression. This software controls from the print speed, up to the coordinates X, Y, Z [3].

That is why knowing the mechanical properties of the pieces manufactured with new materials are one of the most important factors to develop this technology. In the case of Timberfill it is interesting especially for its appearance, both visual and tactile, thereby it seems wood texture. This material can be used in different industry fields.

Flexural test (four points bending) is an application by using two precise loads and two support points. The application of these forces causes the bending on the pieces. These pieces able to bend in a wide range of radius or break quickly based on the various printing parameters [3].

2.1. Additive manufacturing methods

Additive Manufacturing technology is based on the deposition of material, usually layer-to-layer to manufacture a piece designed in CAD software.

Initially, the piece is designed using Solidworks software, then transferred to another software called Simplify 3D which makes a connection between the CAD program and the manufacturing machine (printer).

Following the first criterion of additive manufacturing classification: liquid, solid or powder. Each one of them contributes different properties, being possible to use them in different printing methods.

The second way to classify them is according to ASTM Standard, which divides them into the following groups: Material Extrusion, Material Jetting, Vat Photo polymerization, Binder Jetting, Sheet Lamination, Power Bed Fusion and, finally, Directed Energy Deposition [4].

2.2. FFF technology

Fused Filament Fabrication (FFF) is one of the most typical AM methods. Only can be called Fused Deposition Manufacturing (FDM) in case a Stratasys printer is being used.

This kind of machine (Fig. 1) manufactures 3D objects by adding layer upon layer. A filament as initial state of the material is placed on the printer. Then 2 feed rollers take the filament and forces into the heater, preheating the material in order to reach the pre-selected temperature. Finally, the printer deposits the semi-melted material onto the hot bed and immediately hardens to withstand the next layer.

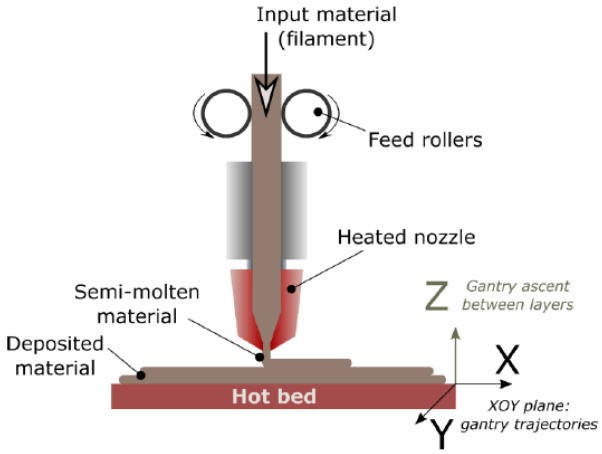

Figure 1: Overview of the FFF printer [5]

Pyramid 3D studio is the printer used as in previous projects [6, 7]. This printer allows the movement of the head in the X and Y axes, while the displacement on axis Z is performed by means of the hotbed.

There are several printing parameters that can influence on the mechanical properties of parts manufactured by FFF. Changing these parameters to achieve the best combination to obtain a better flexural performance is main scope of this study. Several different parameters that can be modified, like the following: *layer height, nozzle diameter, printing speed, infill pattern, fill density, and printing orientation.*

2.2.1. Layer height

Layer height is one of the most influence parameters which control the overall height of the layers. As can be seen in (Fig. 2) it establishes the height of each layer determining the amount of layers that should be in order to finish the part.

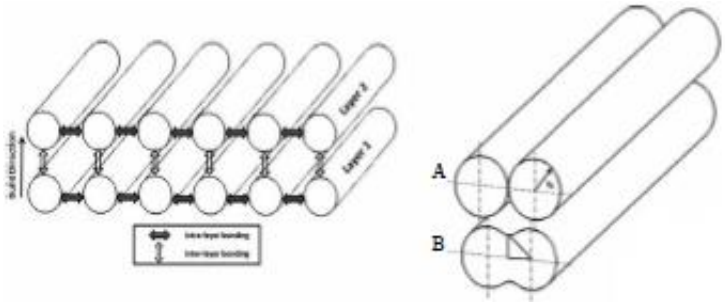

Figure 2: Clarifying layer height [8]

B.M. Tymrak et al.[9], concluded the result for layer heights, tensile strength averages varied by 11.9 MPa, or 22%, between 0.3 mm and 0.2 mm layer heights while elastic modulus varied by 194 MPa, or 6%, between 0.4 mm and 0.2 mm layer height on PLA. On the other hand R. Jerez Mesa et al. [10], shown that the layer height has the most significant impact on fatigue life for PLA so that increasing the layer height, better results of number of cycles have been obtained until failure.

2.2.2. Nozzle diameter

The diameter of the nozzle is another important parameter to take into account because it can influence on infill strategies. It is also important due to the intrinsic characteristics of Timberfill material, composed by wood fibers.

Giovanni Gomez-Gras et al.[5], proved that there is a strong relation between the infill pattern, density, and nozzle diameter as the best combination obtained from the results for fatigue performance of PLA material.

2.2.3. Infill pattern

Infill strategies are determined by the nozzle diameter and can be divided into two different parameters (infill pattern and fill density). There are some different infill patterns such as (rectilinear, linear, grid, triangular, honeycomb etc) as showed in (Fig. 3).

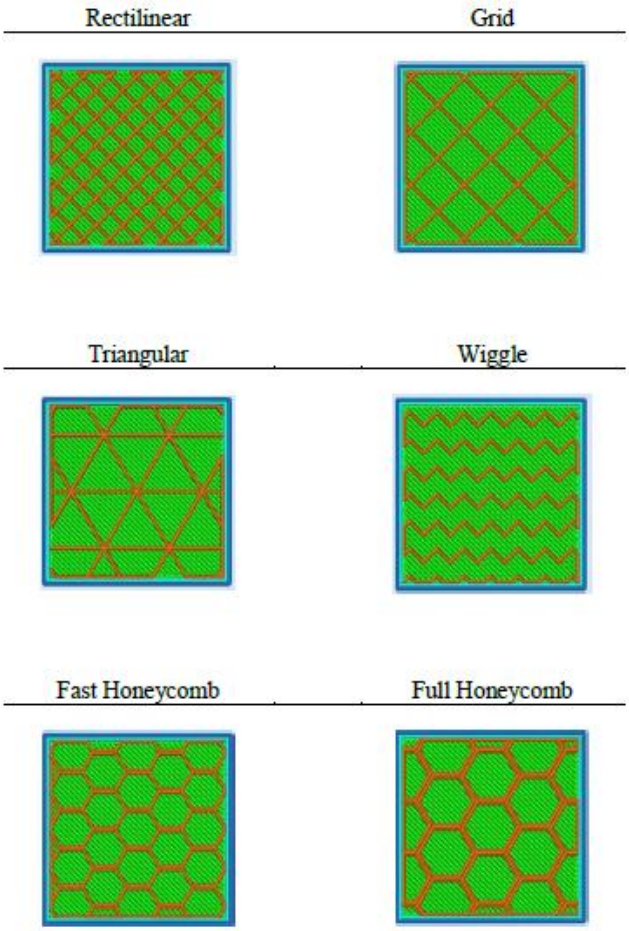

Figure 3: Infill patterns [11]

2.2.4. Fill density

Filling density indicate the percentage of solidity of inside the piece. A 100% filling printed part should be a totally solid piece, whereas a piece with a 0% filling is completely empty. Some various infill percentage is shown in (Fig. 4).

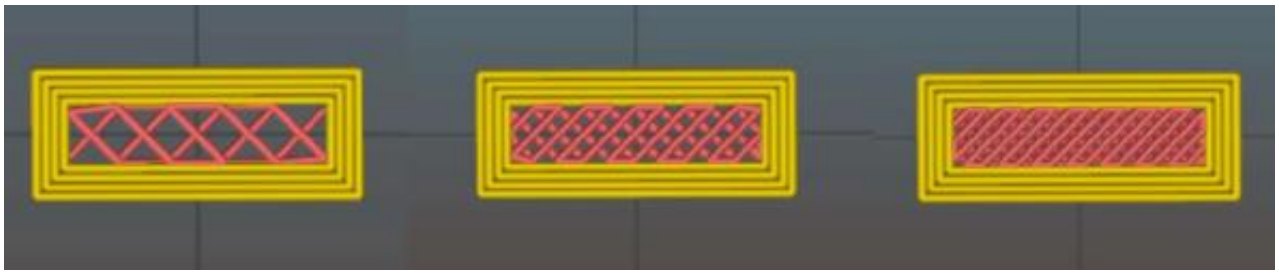

Figure 4: Infill percentages 25%, 50%, 75%. [12]

2.2.5. Printing velocity

There are different speeds to modify to print the parts. The most important phase are the first layer printing speed and the printing speed of the sample.

First layer velocity plays a vital role to obtain the piece correctly, because it should be attached onto the hotbed completely. If this speed is too high, the semi-meld material will not be fixed onto the base and the piece cannot be made correctly.

2.2.6. Printing orientation

Printing orientation also known as building orientation must be taken in account to select as printing parameters. (Fig. 5) shows different building orientations of specimens according to the origin in the FFF machines.

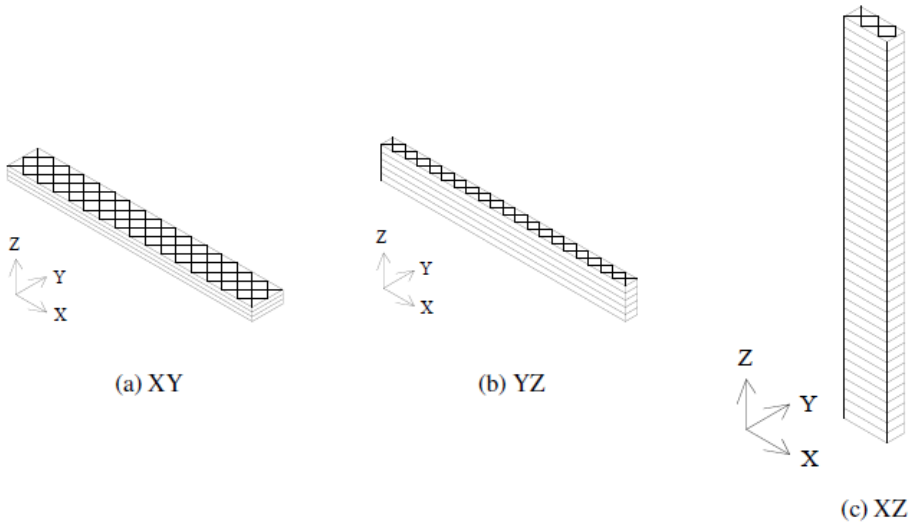

Figure 5: Different printing orientation [13]

According to ASTM Standard exist two types of test based on deformation rate of the sample. Firstly, the printing orientation must be chosen in order to conduct experiments.

According to the literature [14], several studies have been conducted with the aim of studying the influence of process parameters on the strength of parts fabricated with the most important additive manufacturing technologies.

2.3. Materials

There are different kinds of material could be used in this technology including, thermoplastics, photopolymers, etc. But, polymers in thermoplastics category play an important rule due to their presence in greatest market penetration and user accessibility. There are a number of polymeric materials available from machine manufacturers and choices are dependent on the methodology used to create objects such as Acrylonitrile Butadiene Styrene (ABS), Polycarbonate (PC), Polylactide (PLA), Toughened Polystyrene, Nylon, Toughened Polycarbonate, and Polyurethane. In the other hand, equipment manufacturers offer materials that perform at high temperatures, and are chemically resistant such as Polyphenylene Sulfide (PPS), Polyetherimide (PEI), Polyphenylsulfone (PPSU), and Polyether Ether Ketone (PEEK).

Several works have been done on material characteristics of PC [15], and some comparison research between ABS and PLA [16, 17, 18, 19], moreover some other materials [20].

In this project, the specimens are preparing with Timberfill "Champagne" (2.85 mm) as shown in (Fig. 6) developed and manufactured by company Filamentum located in the Czech Republic. This material was developed by that firm with a purely aesthetic purpose that of imitating objects with a wood aspect. To achieve that objective, the company developed a composition of biodegradable PLA polymer combined with wood fibers in a 90% -10% ratio approximately. It is provided as a commodity material, with the purpose of becoming a commonly used material in FFF machines for various applications. However, it is essential characterize and understand the performance of FFF-processed Timberfill parts. Input technical information provided by the manufacturer is indicated in (Fig. 7).

Figure 6: Timberfill champagne spool [21]

Physical properties	Typical Value	Test Method	Test Condition
Material density	1,26 g/cm³		20 °C
Melt volume index	25 cm³/10 min	ISO 1133	190 °C, 2,16 kg
Diameter tolerance	± 0,10 mm		
Weight	750 g of filament (+ 250 g spool)		

Mechanical properties	Typical Value	Test Method	Test Condition
Tensile strength	39 MPa	ISO 527	at break, 5 mm/min
Elongation at break	2 %	ISO 527	5 mm/min
Tensile modulus	3200 MPa	ISO 527	1 mm/min
Charpy impact strength	22 kJ/m²	ISO 179/1eU	23 °C, unnotched
Hardness	77 Shore D	ISO 7619	

Thermal properties	Typical Value	Test Method	Test Condition
Melting temperature	145–160 °C		
Heat distortion temperature	48 °C	ISO 75	method B, 0,45 MPa

Printing properties	Typical Value	Test Method	Test Condition
Print temperature	170–185 °C		
Hot pad	40–50 °C		

Figure 7: Technical data sheet developed by manufacturer [21]

2.4. Mechanical properties

The mechanical behavior of 3D printed parts is one of the most difficult properties to define in this kind of parts, for two main reasons. Firstly, because of the high number of parameters to control during the additive process, which makes it complex to analyze. Secondly, because of the high anisotropy that this kind of parts show when tested, which is defined by their manufacturing history as the resistance of the raw material and the cohesive forces between bonded layers interact in a complex way [14]. Mentioning to the bibliographical references, a number of studies have investigated the mechanical properties of printed parts through FFF process in variable strategies on different materials.

3. Manufacturing design

The main influential parameters on the flexural performance of Timberfill material were selected based on previous projects [6, 22] to perform the experimental design. For this task, the selected factors and levels for Taguchi experimental design are shown in (Table 1). After deciding what are the four most important parameters, the values of the parameters should be combine each other with all the possible combinations. Therefore, should be carried out 3^4 combinations to cover each one of the cases. This partial DOE method allows to combine numerous factors and levels and reduce the number of experiments drastically, to assess the influence of a broad parameter combination. The main objective is to find the most significant manufacturing parameters of the parts, to increase their fatigue life.

Table 1: Factors and levels used for the DOE.

Factors	**Code**	**Levels**		
		1	2	3
Layer height [mm]	A	0.2	0.3	0.4
Nozzle diameter [mm]	B	0.5	0.6	0.7
Fill density [%]	C	25	50	75
Printing velocity [mm/sec]	D	25	30	35

These factors have been selected for their high influence on mechanical properties of rapid manufactured parts, as reviewed in the state of the art, and their levels have been selected according to previous experience of research group, manufacturer data sheet recommendations and observations in a preliminary experimental phase. The assignment of the factors and interactions is performed using the linear graph corresponding to the orthogonal array (Fig. 8) to avoid a possible confusion between factors and interactions.

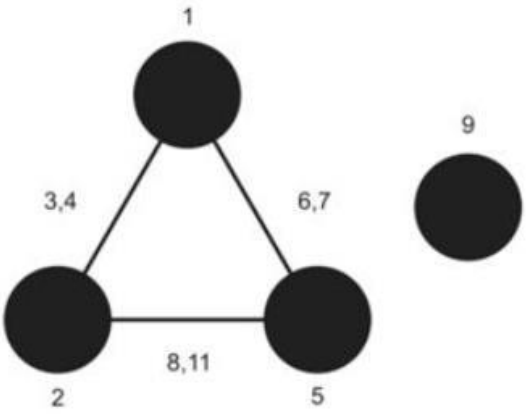

Figure 8: Linear graph of orthogonal array [22]

Each of the points on the graph represents a factor and the lines the interactions between them. The number in each of them represents the column which is assigned. As we are interested to investigate, the effect of the manufacturing parameters and their interactions, factors A, B and C were assigned to the nodes/columns 1, 2 and 5 respectively. The resulting factor is assigned to column 9.

To analyze the influence of these factors an L27 Taguchi orthogonal array has been selected to conduct the experimental phase shown in (Table 2).

Table 2: L27 Taguchi orthogonal array for the DOE

	A	B	C	D
BH-#1	0.2	0.5	25	25
BH -2	0.2	0.5	50	30
BH -3	0.2	0.5	75	35
BH -4	0.2	0.6	25	35
BH -5	0.2	0.6	50	30
BH -6	0.2	0.6	75	25
BH -7	0.2	0.7	25	35
BH -8	0.2	0.7	50	25
BH -9	0.2	0.7	75	30
BH -10	0.3	0.5	25	30
BH -11	0.3	0.5	50	35
BH -12	0.3	0.5	75	25
BH -13	0.3	0.6	25	35
BH -14	0.3	0.6	50	25
BH -15	0.3	0.6	75	30
BH -16	0.3	0.7	25	25
BH -17	0.3	0.7	50	30
BH -18	0.3	0.7	75	35
BH -19	0.4	0.5	25	35
BH -20	0.4	0.5	50	25
BH -21	0.4	0.5	75	30
BH -22	0.4	0.6	25	25
BH -23	0.4	0.6	50	30
BH -24	0.4	0.6	75	35
BH -25	0.4	0.7	25	30
BH -26	0.4	0.7	50	35
BH -27	0.4	0.7	75	25

It should be mention that, all of specimens are printed only in honeycomb infill pattern.

3.1. Specimen fabrication

The samples have been manufactured according to ASTM D6272 Standard [23]. This test method covers the determination of flexural properties of unreinforced and reinforced plastics, including high-modulus composites and electrical insulating materials in different forms. These test methods are generally applicable to rigid and semi rigid materials. However, flexural strength cannot be determined for those materials that do not break or that do not fail in the outer fibres. This test method utilizes a four point loading system applied to a simply supported beam [23]. Regard to this method at least five specimens shall be tested for each sample in the case of isotropic materials or molded specimens. The specimens may be cut from sheets, plates, or molded shapes, or may be molded to the desired finished dimensions. The actual dimensions used are shown in (Fig. 9).

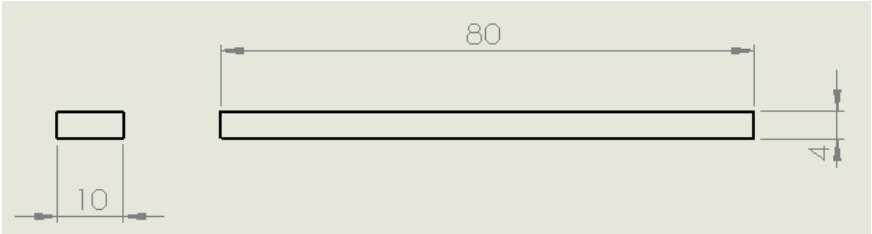

Figure 9: Dimensions of test specimens: 80 x 10 x 4 mm, [23]

The CAD software using to design the sample is SolidWorks, and then the drawings are transferred to the 3D simplify software to slice the sample layer by layer and apply the printing configurations. All the specimens are printed using Pyramid studio 3D printer shown in (Fig. 10).

Figure 10: Pyramid studio 3D printer [6]

The parameters that are not object of study such as building orientation, raster angle, temperature, etc., have been kept constant among different specimens.

The cross section of the sample is shown in (Fig. 11) that indicates that the thickness of outlines of the specimen should be 1.2 mm. To achieve this specific shape due to the selected parameters, the best prudence is modified as can as possible explained following.

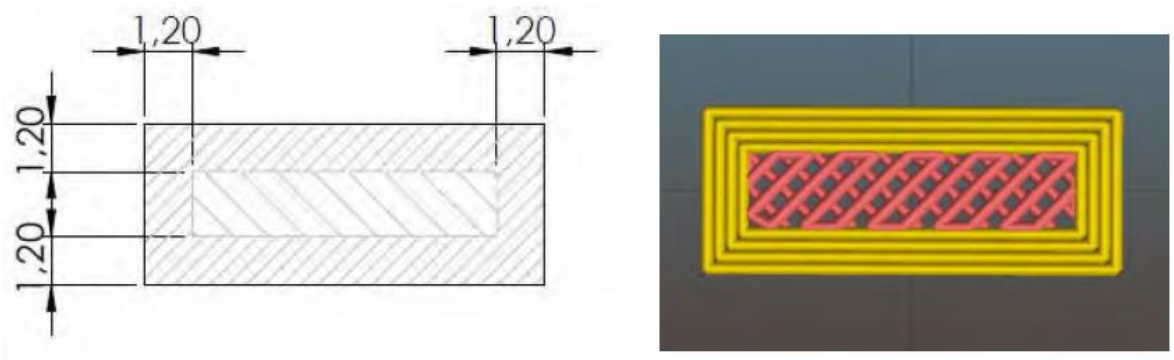

Figure 11: Plan of the cross section [6]

As already mentioned the selected layer heights are 0.2, 0.3, and 0.4, (mm) so to execute the accurate thickness of bottom and top partition of the samples by multiply the numbers of layer height, the numbers of 6, 4, and 3 are determined for each one of the chosen layer heights respectively in the configuration of the printing process as shown in (Fig. 12). In the other side for the diameter of the nozzle due to the property of the material are selected in three different levels (0.5, 0.6, 0.7) (mm). Hence, rely on the nuzzle diameter of 0.6 mm multiply by 2 layers to obtain 1.2 mm thickness of outline walls, for the other diameters of the nozzle only 2 layers are constant because there is no right proportion between the thickness and the diameter of all nozzles.

Another point that should be taken into account is that, while printing all five samples at the same time the infill pattern was not similar for all of them as it can be seen from (Fig 12), so for this reason the specimens are printed one by one in the constant position.

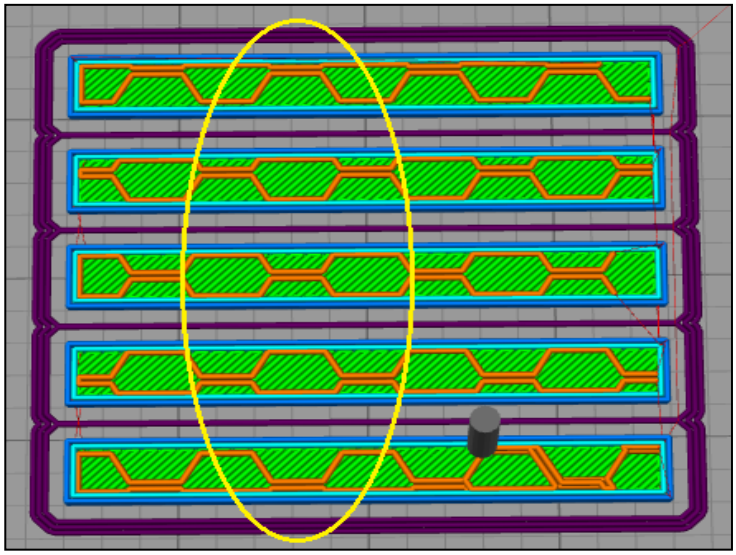

Figure 12: Different infill shape of 5 samples

To ensure that the material is extruding nicely and lying on the bed correctly before the actual printing of main model 3 skirt outlines to the beginning of each print is added by 2mm offset from the part.

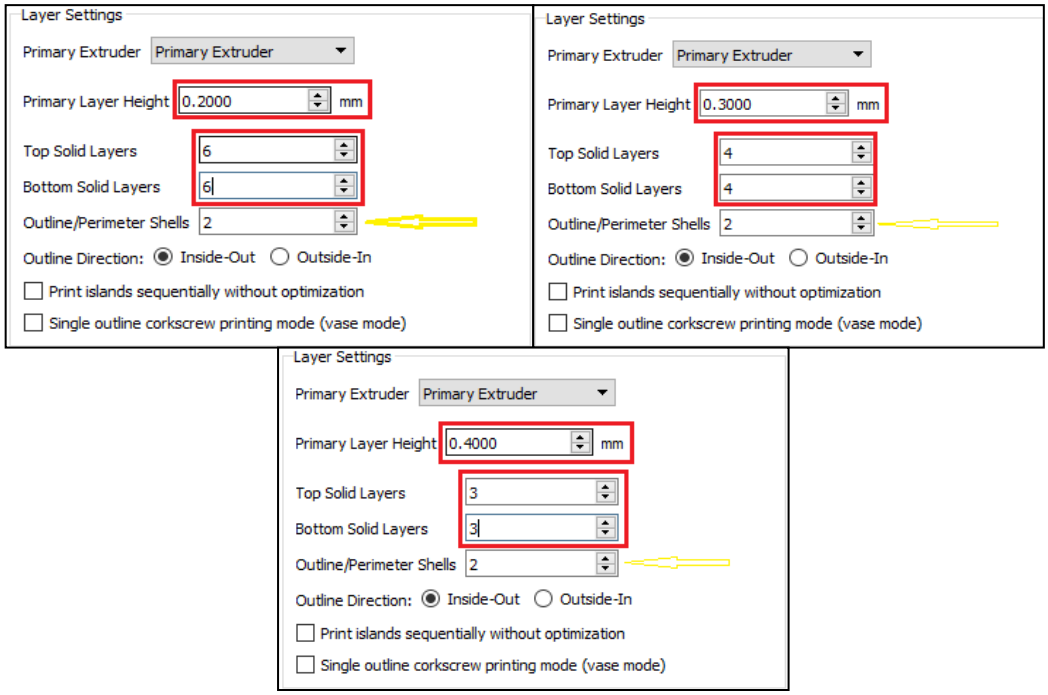

Figure 13: Primary and solid bottom and top determined layers

Based on the statements mentioned above, the cross section of different percentages of infill density and the main sample printed are shown in (Fig. 14).

Figure 14: Specimens printed with 25%, 50%, 70% infill density and the sample on the printer's bed

3.2. Metrology

To achieve more accuracy of the tests results, the dimensions of all 130 specimens have been measured in four different points based on the standard and the average magnitudes are calculated for length, width, and thickness (Fig.16). With this information the actual area of the section of each specimen could be in particular. The data will be used later to calculate the stresses generated on the specimens.

In the other side, the specimens were weighed individually to calculate the density and find correlations between the amount of extruded material for each specimen and printing parameters.

The measuring instruments used for this task:

- Vernier caliper with 10 µm resolution, length of specimens.
- Micrometer with 1 µm resolution, Width and thickness of the specimens.
- Scale with 1 mg resolution, weight of the specimens.

Sample	TIMB-B-H-#1-1		
Operator	Marc Mimbrero Gallardo		
Width (µm)	Thikness(µm)	Length (mm)	Weight (mg)
10342	4062	80.08	2.849
10350	4034	80.04	
10463	3936	80.07	
10331	3885		

Observacions

	Average	Error	Desviació	
Width (µm)	10371.5	98.9	61.5	
Thikness (µm)	3979.3	132.9	82.9	
Length (mm)	80.1	0.1	0.0	
Section (mm^2)	41.2708	1.4329	Er (%)	3.5%
weight (mg)	2.8	#DIV/0!	#DIV/0!	
Density (g/cm^3)	0.001	#DIV/0!		

Version 20-02-17	Resolució	
	Thikness (µm)	1
	Length (µm)	10
	Weight (mg)	1

Figure 15: Template of metrology. Source: DEFAM

3.3. Test machine and procedure

Flexural tests on the fabricated samples were performed according to the ASTM D6267-02 [23]. This test method covers the determination of flexural properties of unreinforced and reinforced plastics, including high-modulus composites and electrical insulating materials in the form of rectangular bars molded directly or cut from sheets, plates, or molded shapes. This test method is generally applicable to rigid and semi-rigid materials and utilizes a four point loading system applied to a simply supported beam D.

These experiment tests were conducted using all-round-line Table-top machine (*ZwickRoell Z020, GmbH, Germany) as shown in (Fig. 15).* The technical information is mentioned as follow:

- *Equipped with a 500 N load cell*
- *Displacement rate of 19 mm/min*
- *Maximum displacement was set at 10 mm*
- *No preload was applied*

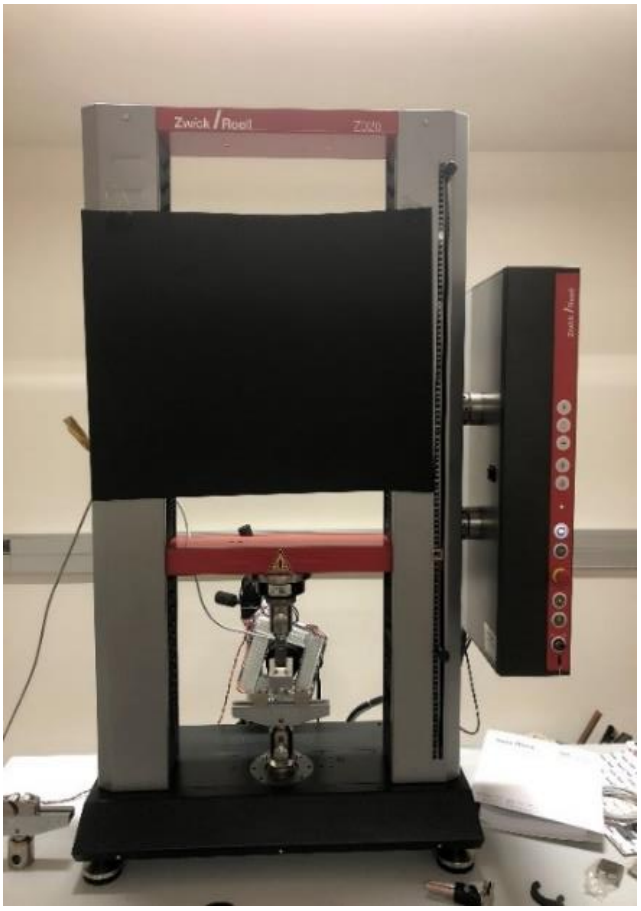

Figure 16: Universal material testing machine, zwick roell Z020 [22]

A bar of rectangular cross section rests on two supports and is loaded at two points (by means of two loading noses), each an equal distance from the adjacent support point. The distance between the loading noses (the load span) is either one third or one half of the support span (Fig.16). A support span-to-depth ratio of 16:1 shall be used.

The loading noses and supports shall have cylindrical surfaces. In order to avoid excessive indentation or failure due to stress concentration directly under the loading noses, the radii of the loading noses and supports should be 5 ± 0.1 mm. regarding to this method the distances between support spans and load spans shall be 64 mm and 21.3 mm respectively.

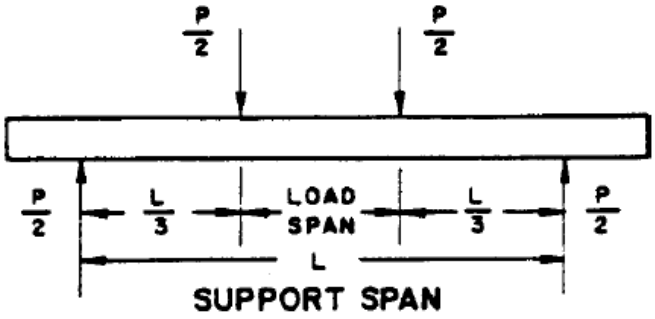

Figure 17: Loading diagram [23]

The arc of the loading noses in contact with the specimen should be sufficiently large to prevent contact of the specimen with the sides of the noses as shown in (Fig. 17).

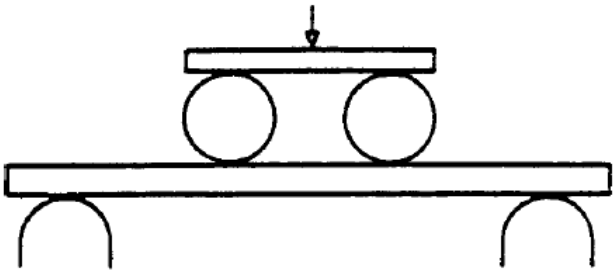

Figure 18: Loading Noses and Supports (Example of One Third of support span) [23]

The rate of crosshead motion is calculated as follow, and the machine is adjusted as near as possible to that calculated rate for the load span of one third of the support span:

$$R = \frac{0{,}185\ Z\ L^2}{d} \qquad (1)$$

Where:

- *R = rate of crosshead motion, mm (in.)/min,*
- *L = support span, mm (in.),*
- *d = depth of beam, mm (in.), and*
- *Z = rate of straining of the outer fibers, mm/mm (in./in.) min. Z shall equal 0.01.*

In no case shall the actual crosshead rate differ from Eq. 1, by more than ± 10 %.

Based on the equation (1), the achieved flexural velocity rate is 19 mm/min. This value is determined for the test machine.

Another relevant aspect is maximum strain in the outer fibers which is 0.05 mm/mm (in./in.), due to the specimens withstand high deformations. It is possible that they do not end up breaking; therefore the norm establishes the test is finished once the maximum deformation of the external fibers has reached.

To calculate the deflection needed to achieve it, the standard provides the following equation:

$$D = \frac{0{,}21\, r\, L^2}{d} \qquad (2)$$

Where:

- *D = deflection, mm (in.),*
- *r = strain, mm/mm (in./in.),*
- *L = support span, mm (in.), and*
- *d = depth of beam, mm (in.).*

Once the conditions are determined we achieve a maximum flexural rate of 10.89 mm.

To validate the procedure with the calculated values, 10 samples were tested before the main samples. The results of this test confirmed the procedure and validated it. Thereby these values were introduced in the setup of the test machine. The values are shown in the table below (Table 3).

Table 3: Experimental setup values

Displacement velocity	19 mm/min
Maximum flexural ratio	10.89 mm

3.4. Experimental setup

First of all, it is necessary to prepare the setup to guarantee the quality of the test. To carry out this test, an external data logger (spider 8) is used to save the applied load in each point. In one side, a 500 N load cell is connected to a DAQ spider that transfers the data to the computer (Fig. 19). In the other hand, this setup consist a set of a HD camera that records the test video at 60 HZ which is also connected to the spider data logger. The camera has equipped with a switch-controlled flash to illuminate the test area and to synchronize the data either as shown in (Fig. 20).

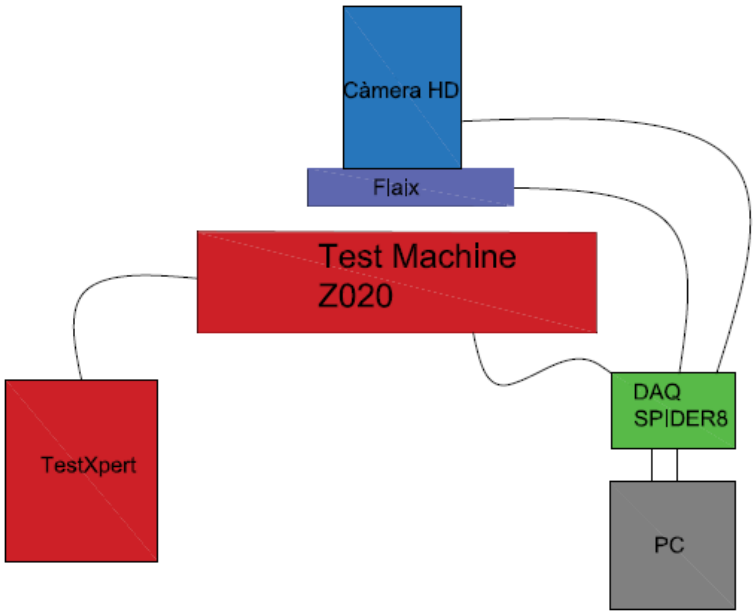

Figure 19: Block diagram of the equipment [22]

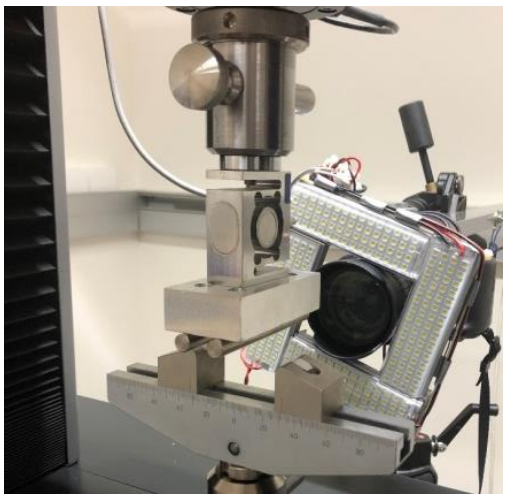

Figure 20: Camera assembly [22]

To embed the samples on the support spans regard to the exact distances and positions, all of the procedure is observed due to the standard.

Once all the setup is adjusted, the tests are carried out for all of the 135 printed specimens (Fig. 21).

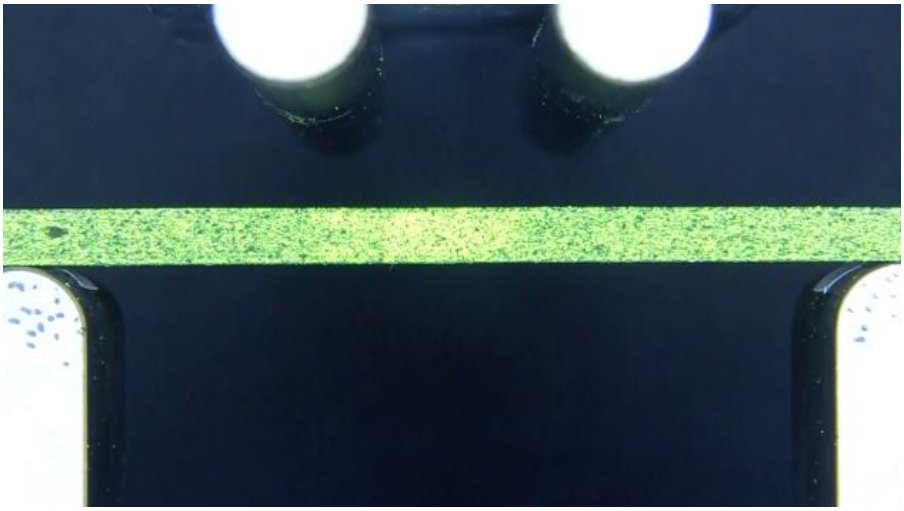

Figure 21: Initial position

4. Analyzing process

A total of 135 samples were tested (i.e. N=5 specimens per group). To obtain the defined mechanical properties in this project such as Young modulus (E), maximum elongation, yield strength (σ_y), resilience modulus (MR), and tenacity modulus (MT) Matlab program (Matlab R2018b, The MathWorks Inc.) is used to analyze the data.

When each test is finished, two different files are generated. First an (*.asc)* type that contains the force collected from the load cell and recorded voltage versus time. Second the video recorded by the camera.

First of all, the video and the recorded data have to be synchronized. It is been done by means of a Matlab script. When the test starts, the flash is activated and sends a 0V signal to the Spider to start recording data. Subsequently, this Matlab script synchronizes the dark frame of the video and the spider data recorded alongside the time that the test has been. In (Fig. 22) a drawing of this process can be seen.

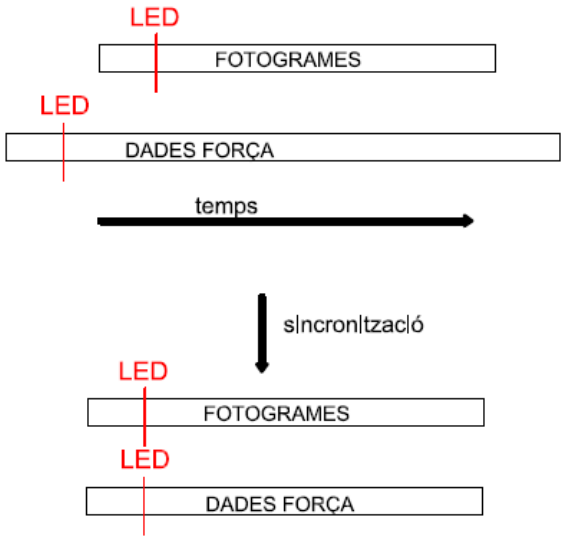

Figure 22: Drawing of the synchronize [6]

In the first step of analyzing, the HD video should be separated to obtain each photo frames. Since the camera captures 60 frames per second and the average duration of the test is 50 second, the average frames of each video file shall be 3000. Then, the video file with the frames is synchronized by Matlab scrip. In this step the Matlab detects the points until the maximum bending position before the sample will be broken.

A grid is generated in the initial frame of the test sample; this gridding consists of a straight line divided by 50 points at the outer fiber and two rectangular grids at the support spans (Fig. 23). It is important that the linear grid occupy approximately the space from center to center of the two load spans, the point which the maximum deflection occurs.

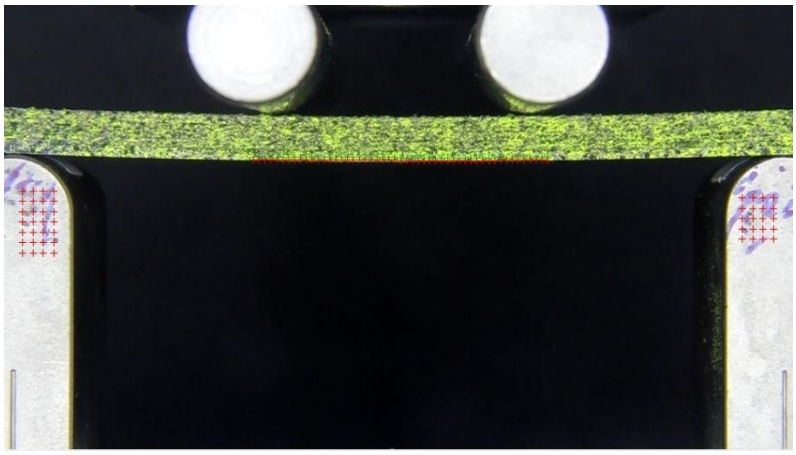

Figure 23: Generated grids

In this step the marked pixels are tracking and the deflection is calculating consequently based on the differences between the initial and final position. The results convert to an array at the X-axis and Y-axis separately. The difference between the positions in the current frame (in red) and the starting position (in green) is shown in (Fig. 24).

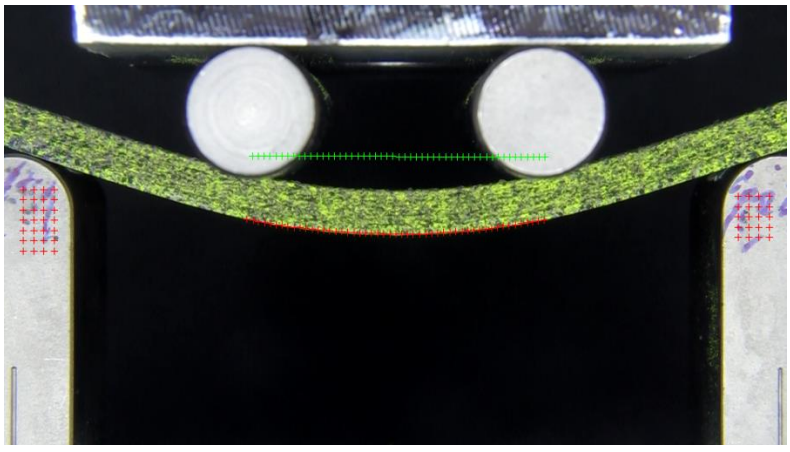

Figure 24: Image processing

By finishing of this process, two scroll files have been generated which can be used for the deflection script to transfer the scroll values of the points into real deformations of the outer fiber.

Next the pixels that Matlab has measured should be converted in millimeters. So, GIMP 2.10.8 software is used to do this as it can be seen in (Fig. 25).

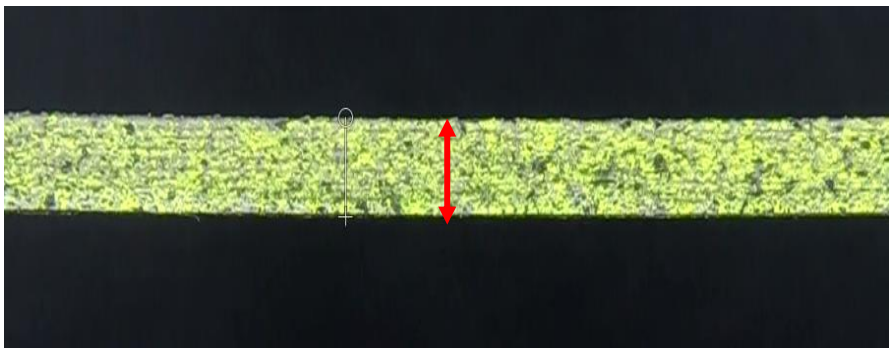

Figure 25: calculating Pixel/mm ratio

The deformation is calculated from deflection value using the following equation:

$$r = \frac{d\ D}{0{,}21\ L^2} \qquad (3)$$

Where:

- *r= Deformation (mm)*
- *d= Deflection (mm)*
- *L= Distance between support spans (64 mm)*
- *d= Samples thickness (mm)*

The thickness and L value of each specimen is entered manually.

By means of another Matlab script, the voltage and the deformation are calculated for the specimen second by second and the results are synchronized with the deformations value that have been calculated previously. Finally a .txt format file is generated with voltage, deformation versus time. Consequently, the tension is calculated by the following equation:

$$S = \frac{P\ L}{b\ d^2} \qquad (4)$$

Where:

- *S= Tension applied to the external fiber (MPa)*
- *P= Force (N)*
- *b= Width (mm)*
- *d= Thickness (mm)*

Here the average value of thickness and width are defined manually due to the measurements that have been done before the test.

Finally, the obtained file is exported to the template Excel document which is already prepared to calculate the properties (Fig. 26).

E (GPa)	Err_E (GPa)	$Rp_{0.2}$ (MPA)	$\sigma_{r,e}$ (MPa)	e_{max} (%)	MR (MPa)	MT (MPa)
1.74	0.0013070004273	26.87	32.39	3.92	0.25393	0.648

e	σ (MPa)
0	0.037255
5.1E-05	0.063091
2.3E-05	0.087197
0.000105	0.099425
0.000121	0.125256
8.1E-05	0.149935
0.000112	0.186432
0.000133	0.21283
0.000164	0.249051
0.000196	0.273555
0.000241	0.312287
0.000188	0.348471
0.000231	0.373019
0.000233	0.411745
0.000258	0.447892
0.000278	0.472483
0.000296	0.511202
0.000415	0.547763
0.000311	0.584366
0.000271	0.623077
0.000328	0.659639
0.000379	0.696248
0.000428	0.734953
0.000432	0.771514
0.000441	0.808131
0.000463	0.84762
0.000487	0.895808
0.000509	0.932431
0.000536	0.971123
0.000545	1.007684
0.000549	1.044314
0.000579	1.082998
0.000603	1.120193
0.000673	1.168615
0.000668	1.207292
0.000704	1.243854
0.000713	1.280497
0.000769	1.319168
0.000787	1.355729
0.000823	1.392901
0.000808	1.443876
0.00083	1.480437
0.000866	1.517638
0.000884	1.56817
0.000915	1.604731

Versió

11/05/2017

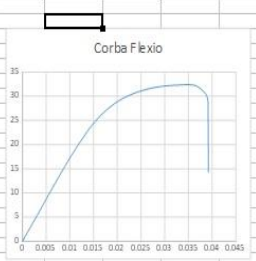

	E (GPa)						$Rp_{0.2}$ (MPA)			N	tp (95%)
	1738.0837	1739.6211	1741.8496	1742.3595	1742.3595	1742.3595	0.9999786			1	12.7062
	Error	Error	Error	Error	Error	Error	1742.3595	-3.5161518	Area	2	4.30265
Extrem	0.000393	0.0003787	0.0003768	0.0003749	0.0003749	0.0003749	0.0231084	891.92603		3	3.18245
Inici	1	34		38		38	666	11.3153		4	2.77645
Final	1261	361	344		344		26.881509	30		5	2.57058
		0.000393		0.0004094		0.0004094	3.5534068	1		6	2.44691
		0.0003939		0.0004101		0.0004101	3.4903825	2	2.559E-06	7	2.36482
	1.8881867	0.0003958		0.0004122		0.0004122	3.5632746	3	-2.104E-06	8	2.306
	0.6133219	0.0003962		0.0004122		0.0004122	3.4326291	4	7.652E-06	9	2.26216
	0.3314242	0.0003959		0.0004121		0.0004121	3.4305823	5	1.797E-06	10	2.22814
	0.4378127	0.0003954		0.0004117		0.0004117	3.5249557	6	-5.504E-06	11	2.20099
	0.3676576	0.0003973		0.0004136		0.0004136	3.5074396	7	5.214E-06	12	2.17881
	0.2832817	0.0003994		0.0004159		0.0004159	3.497248	8	4.192E-06	13	2.16037
	0.208445	0.0004015		0.0004182		0.0004182	3.4794559	9	7.159E-06	14	2.14479
	0.1571518	0.0004033		0.0004203		0.0004203	3.4482044	10	8.362E-06	15	2.13145
	0.1208798	0.0004039		0.0004211		0.0004211	3.4085302	11	1.318E-05	16	2.11991
	0.1328649	0.0004015		0.0004186		0.0004186	3.5370593	12	-1.751E-05	17	2.10982
	0.1147811	0.0004032		0.0004202		0.0004202	3.4866858	13	1.551E-05	18	2.10092
	0.1063948	0.0004052		0.0004224		0.0004224	3.5219271	14	7.848E-07	19	2.09302
	0.0948129	0.0004072		0.0004246		0.0004246	3.5145151	15	1.075E-05	20	2.08596
	0.083554	0.0004094		0.0004269		0.0004269	3.5042589	16	9.204E-06	21	2.07961
	0.0742365	0.0004117		0.0004294		0.0004294	3.5116154	17	8.853E-06	22	2.07387
	0.0757622	0.0004139		0.0004318		0.0004318	3.3408357	18	6.301E-05	23	2.06866
	0.0759509	0.0004019		0.0004184		0.0004184	3.558644	19	-5.887E-05	24	2.0639
	0.0906212	0.0004027		0.0004188		0.0004188	3.6670494	20	-2.415E-05	25	2.05954
	0.0872486	0.0003905		0.0004029		0.0004029	3.6042969	21	3.656E-05	26	2.05553
	0.0790081	0.0003869		0.0003977		0.0003977	3.5520456	22	3.458E-05	27	2.05183
	0.0707967	0.0003877		0.000398		0.000398	3.505375	23	3.506E-05	28	2.04841
	0.0641779	0.0003899		0.0004003		0.0004003	3.5349665	24	3.013E-06	29	2.04523
	0.0588466	0.0003915		0.0004016		0.0004016	3.5559023	25	7.108E-06	30	2.04227
	0.0540294	0.0003919		0.0004015		0.0004015	3.5570594	26	1.821E-05	31	2.03951
	0.0496629	0.0003923		0.0004011		0.0004011	3.5634308	27	2.092E-05	32	2.03693
	0.0457436	0.0003921		0.0004001		0.0004001	3.5617219	28	2.011E-05	33	2.03452
	0.0421675	0.0003919		0.000399		0.000399	3.5533702	29	2.57E-05	34	2.03224
	0.039178	0.0003923		0.0003987		0.0003987	3.5742499	30	8.905E-06	35	2.03011
	0.0368847	0.0003909		0.0003959		0.0003959	3.6039105	31	4.104E-06	36	2.02809
	0.0344884	0.0003858		0.0003882		0.0003882	3.5903237	32	3.191E-05	37	2.02619
	0.032248	0.0003821		0.0003824		0.0003824	3.5857021	33	2.644E-05	38	2.02439
	0.0305695	0.0003787		0.0003768		0.0003768	3.5121589	34	8.011E-05	39	2.02269
	0.0286211	0.0003807		0.0003786		0.0003786	3.5595477	35	-5.94E-06	40	2.02108
	0.0269915	0.0003799	0.7896073	0.0003764		0.0003764	3.5333848	36	4.412E-05	41	2.01954
	0.0254061	0.0003809	0.34854	0.0003768		0.0003768	3.5543465	37	1.136E-05	42	2.01808
	0.024442	0.0003804	0.2353667	0.0003749		0.0003749	3.4954454	38	7.279E-05	43	2.01669
	0.0233996	0.0003826	0.1491891	0.0003771		0.0003771	3.5006439	39	2.407E-05	44	2.01537
	0.0226644	0.0003849	0.105574	0.0003793	0.1874932	0.0003793	3.475091	40	4.948E-05	45	2.0141
	0.0214543	0.000387	0.1220257	0.0003816	0.5523478	0.0003816	3.5522014	41	-2.128E-05	46	2.0129
	0.0203445	0.0003866	0.1086366	0.0003798	0.3327851	0.0003798	3.5504305	42	3.217E-05	47	2.01174
	0.0193663	0.0003862	0.0865147	0.000378	0.211582	0.000378	3.5249065	43	5.397E-05	48	2.01063
	0.0184021	0.0003876	0.0725033	0.0003787	0.14184	0.0003787	3.5440761	44	2.777E-05	49	2.00958
	0.0175456	0.0003876	0.0597668	0.0003774	0.1080484	0.0003774	3.5266239	45	4.918E-05	50	2.00856

Figure 26: Excel calculation sheet

5. Results

In (Table. 3) can be seen the results achieved once the test and analyze have been done.

Table 3: Table of results

	E (GPa)	Std. dev.	Rp0,2 (MPA)	Std. dev.	sMax (MPa)	Std. dev.	eMax (%)	Std. dev.
1	2.07	0.08	30.66	0.56	35.34	0.34	2.77	0.34
2	2.13	0.04	33.48	0.77	39.52	1.25	3.49	0.33
3	2.17	0.04	34.19	0.42	41.15	0.88	4.65	1.78
4	2.03	0.08	31.56	0.91	37.82	0.49	3.46	0.08
5	2.12	0.04	31.83	0.97	39.76	0.93	4.35	0.00
6	2.16	0.05	32.96	0.47	40.45	0.64	3.92	0.45
7	2.29	0.15	36.28	0.56	44.17	1.82	4.07	0.68
8	2.41	0.04	38.06	1.17	47.26	0.86	4.24	0.31
9	2.24	0.08	35.73	0.56	45.40	0.99	5.34	1.62
10	1.76	0.07	28.45	1.05	34.29	0.68	3.80	0.32
11	1.89	0.05	29.54	0.81	36.26	0.58	4.70	1.68
12	1.77	0.06	29.56	0.71	36.24	0.64	4.72	1.99
13	1.82	0.07	36.58	1.62	34.94	1.37	3.80	0.73
14	1.87	0.08	29.69	0.52	37.46	0.66	4.07	0.14
15	1.82	0.06	28.97	1.05	35.51	2.40	3.96	0.61
16	1.84	0.07	29.27	1.24	36.64	1.29	4.48	0.44
17	1.91	0.08	29.49	1.07	37.01	1.83	3.86	0.44
18	1.94	0.08	30.40	1.62	40.17	1.67	4.89	0.37
19	1.70	0.09	26.60	1.78	26.04	2.03	3.15	1.76
20	1.81	0.08	27.53	0.31	33.19	0.70	3.62	0.31
21	1.73	0.11	27.74	0.64	35.14	1.43	4.57	0.62
22	1.41	0.08	23.32	1.78	27.05	2.25	3.59	0.76
23	1.69	0.11	27.23	0.94	32.97	2.14	4.04	0.50
24	1.89	0.20	29.43	5.46	35.64	7.74	3.88	0.90
25	1.86	0.03	30.71	0.53	37.99	0.81	4.64	0.24
26	1.91	0.09	31.35	1.21	39.79	1.54	4.79	0.26
27	1.95	0.15	31.09	1.61	40.27	1.23	4.80	0.53

6. Results analysis

In this section, the results are analysed using the ANOVA method to calculate the p-values and achieve the most influential parameter on the following properties:

- Young modulus (E)
- Elastic limit ($Rp_{0,2}$)
- Maximum tension (σ_{max})
- Maximum elongation (ε)

The methodology is the same for all of them. First, the significant factors for are analysed for each responses. It can be seen how these factors affect the responses and the interaction between the responses are clarified.

In order to obtain these results analytically, should be create the p-values of each parameter. Since using a significance level of 5%, for which a parameter to be considered statistically, you should get a p-value less than $\alpha = 0.05$. Hence, a parameter will be statistically significant when $p - value < \alpha$.

6.1. Young modulus

As shown in (Table. 4), the only parameter which does not show a significant effect on the Young modulus is printing velocity. The most influential parameter for this response is layer height followed by nozzle diameter and density.

Table 4: p-values of means, Young modulus

Factor	P-value
Layer height	0.000
Nozzle diameter	0.009
Density	0.056
Printing velocity	0.299

It could be concluded that the statistically influent level of factors are 0.2 mm layer height, 0.7 mm nozzle diameter, but there is not too much difference between 50% and 75% infill density as shown in (Fig. 27).

This graph shows that the layer height results have inverse proportion with Young modulus, but bigger amounts of nozzle diameter and density result higher elastic modulus.

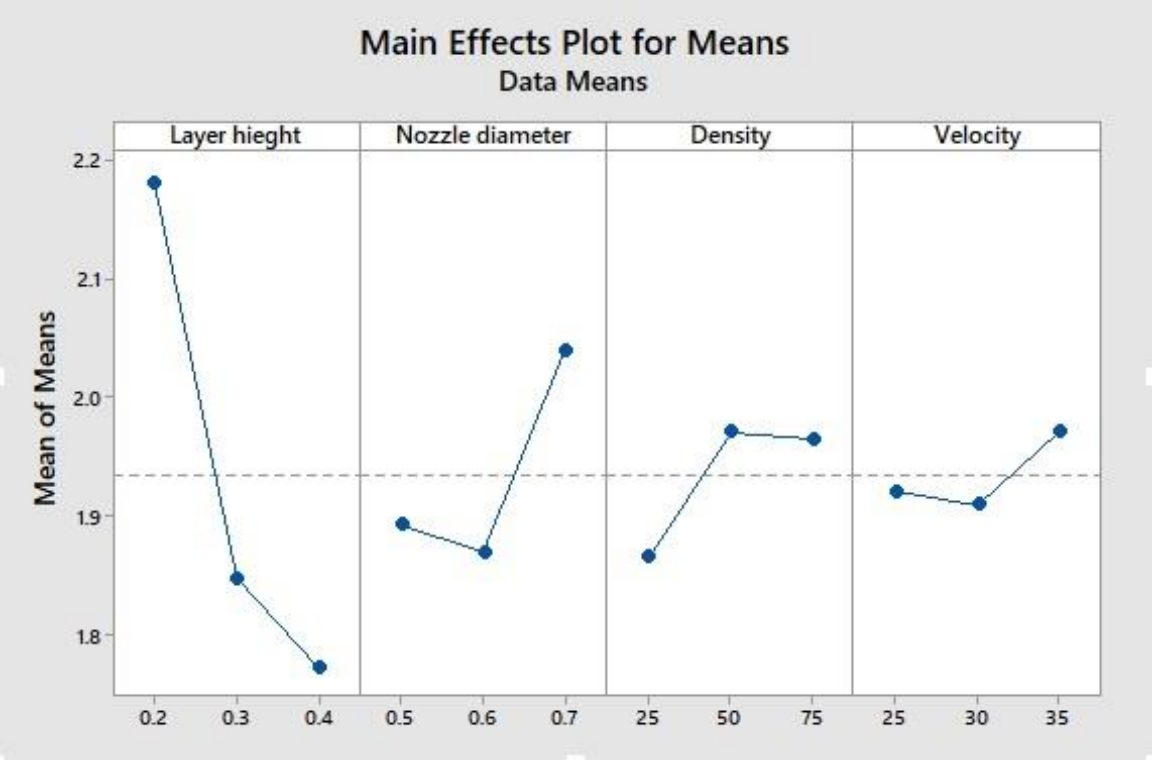

Figure 27: Main effect of means on Young modulus

It is also necessary to observe the interaction between parameters, it means how increasing and decreasing the levels of each factor can effect on the others. It is shown in (Fig. 28), by means of different lines. Each parameter is represented by the lines.

If the lines are parallel between them, it means there is not an interaction between parameters. However, if the lines cross in one or more points it means the parameters could be influential one on each other.

In case of Young modulus (Fig. 28) can be seen how different lines cross as density and nozzle diameter or, for example, layer height and density.

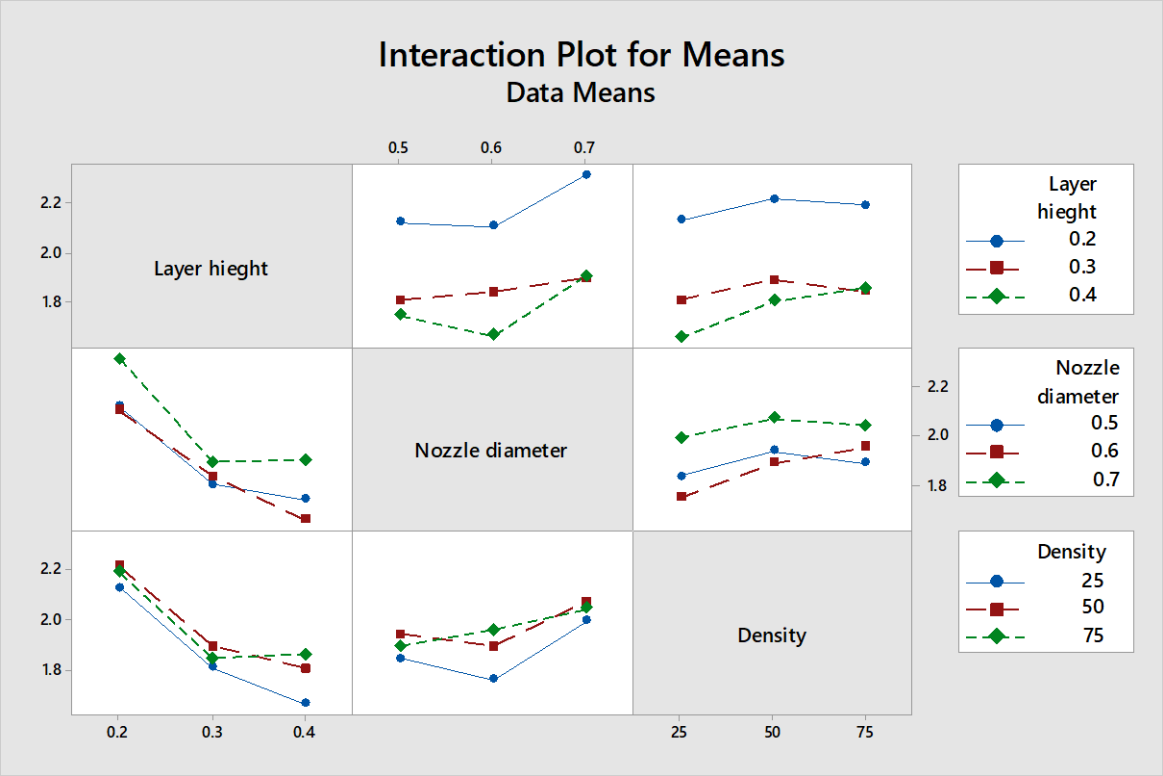

Figure 28: Interaction plot of means on Young modulus

Nevertheless, could be an interaction shown by the interaction plot but the main proof to ensure that the interaction is relevant is (Table. 5). It shows the p-value for the interactions. In Young modulus case, no one of them is relevant.

Table 5: p-value interaction of means, Young modulus

Factor	P-value
Layer height *Nozzle diameter	0.412
Layer height * Density	0.514
Nozzle diameter *Density	0.499

Using Taguchi method also the robustness of the factors can be calculated as signal to noise ratio (S/N) shown in (Fig. 28). Therefore, high S/N values present higher responses and lower variability, and greater robustness of the parameter within the study model. The p-values associated with the S/N of each factor have also been calculated with a 5% significance level ($\alpha = 0.05$).

Those parameters with higher p-values could not be statistically robust. As it can be seen from (Table. 6) the order of significant factors is the same as means effects. But for S/N ratio fill density does not show influence enough regarding that the achieved value of α is higher than 0.05.

Table 6: p-values of S/N ratio, Young modulus

Factor	P-value
Layer height	0.000
Nozzle diameter	0.015
Density	0.067
Printing velocity	0.326

The best selected levels of each factor are shown in (Fig. 29), which indicates that higher robustness achieves by lower layer height but bigger diameter of nozzle which are 0.2 mm, 0.7 mm sequentially.

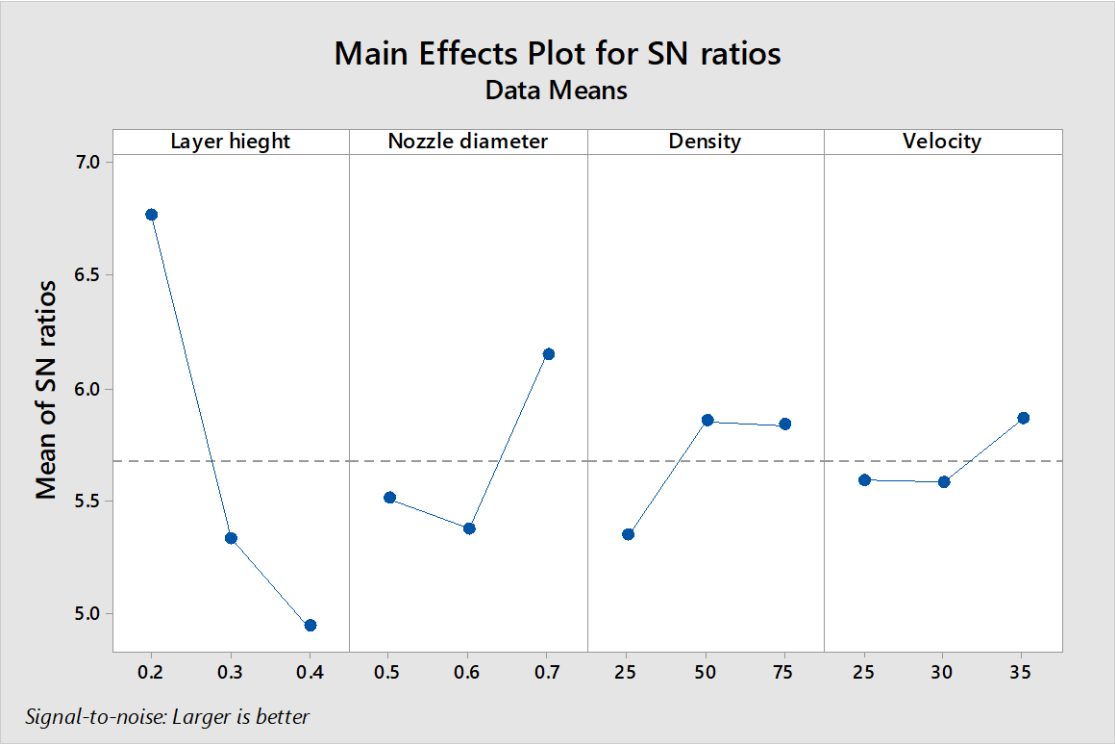

Figure 29: Main plot for S/N ratio, Young modulus

In order to validate the results it is necessary to carry out a statistical study of the residual distribution. The ANOVA analysis is based on the fact that all residues follow a normal distribution.

To perform this assessment ANOVA analysis gives (Fig. 30) which shows the residual plots for mean. In it, can be seen how the points are aligned with the average line in the normal probability plot, while in the histogram we do not get a desired bell shape, although this graph is not far from a normal distribution.

On the other hand, we can observe that there is no trend pattern in the fits and shows a random distribution of points which demonstrate there is not be an error accumulation alongside the tests.

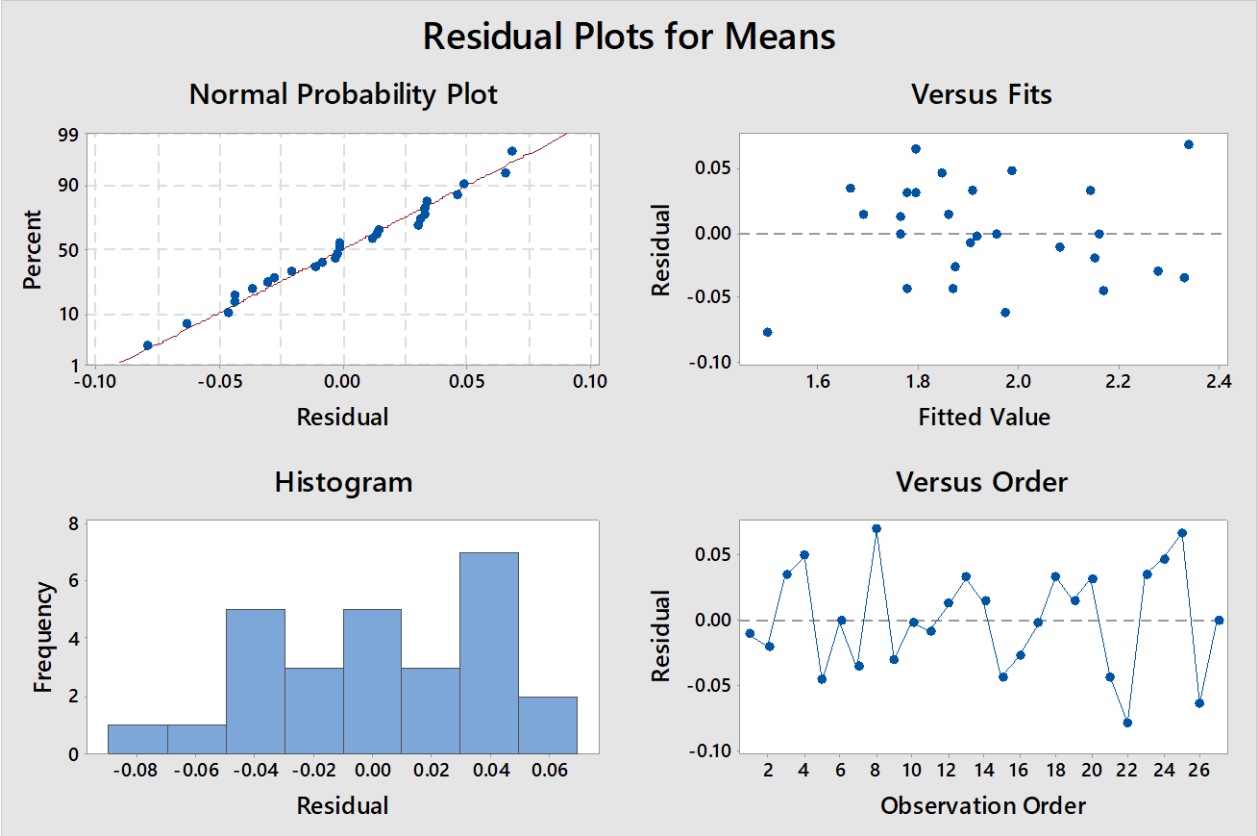

Figure 30: Residual plot for means, Young's modulus

6.2. Elastic limit ($Rp_{0.2}$)

To analyse this property and find the significant parameters, a 5% significance level (α = 0.05) is considered either. As shown in (Table. 7), the only significant factor for elastic limit is layer height.

Table 7: p-values of means, Elastic limit

Factor	P-value
Layer height	0.004
Nozzle diameter	0.065
Density	0.752
Printing velocity	0.288

Consequently, it is necessary to see how the variation of the different factors affect the elastic limit, which is indicated in graph of main effects for the averages (Fig. 31).

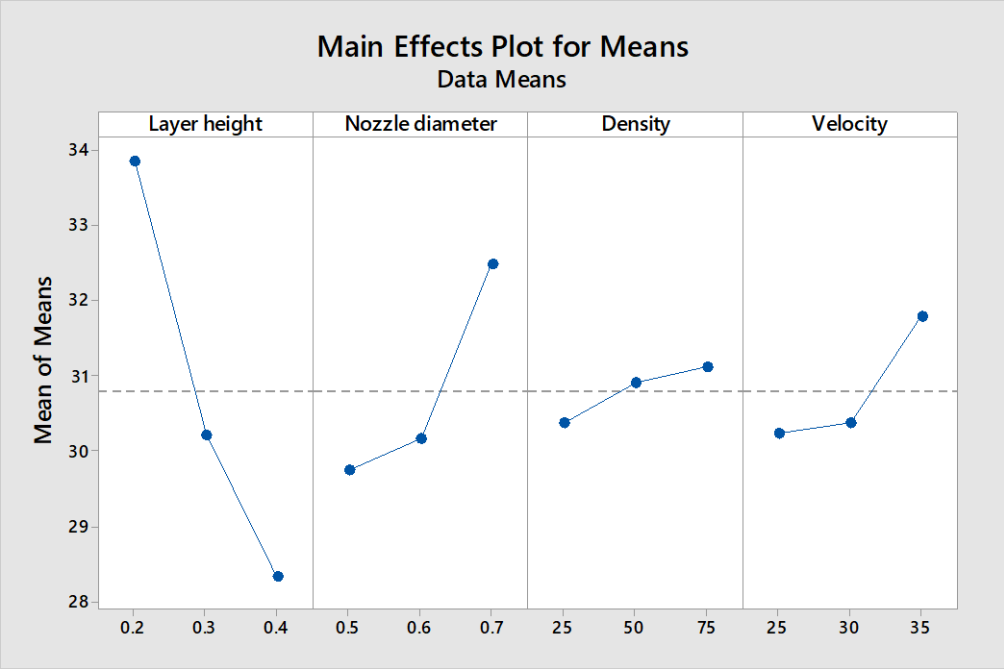

Figure 31: Main effect of means on Elastic limit

As already mentioned the most significant parameter due to the p-value on elastic limit is layer height that it should be lower to obtain the bigger elastic limit which in this project is 0.2 mm. On the other side, the nozzle diameter has a correct proportion with the elastic limit, it means the bigger diameter the higher elastic limit.

Regarding to the interactions between the parameters, it should be taken into account that different cross line between parameters, which could be significant (Fig. 32).

Figure 32: Interaction plot of means on Elastic limit

As in the previous section, we must take a look to (Table. 8). Likewise the previous section, the p-value does not show significant. It means, there is no influential interaction between parameters.

Table 8: p-value interaction of means, Elastic limit

Factor	P-value
Layer height *Nozzle diameter	0.158
Layer height * Density	0.456
Nozzle diameter *Density	0.818

To verify the robustness of the statistical model as already done, it will consider the SN relationship (signal to noise), the ratio between the value of the output signal of each parameter and the noise or error of this model.

To determine the robustness of each factor in the face of possible external variability, the p-value is checked by establishing a 5% significance level (α = 0.05) (Table. 9).

Table 9: p-values of S/N ratio, Elastic limit

Factor	P-value
Layer height	0.004
Nozzle diameter	0.074
Density	0.669
Printing velocity	0.296

The only influential factor on the S/N ratio for the elastic limit is layer height, but to achieve the higher elastic limit, the best level of each paraemter are shown in (Fig. 33), that are 0.2 mm height of layer, 0.7 mm diameter of extruder, and printing speed of 35 mm/s. but the result shows that the variation of the density does not effect on the elastic limit significantly.

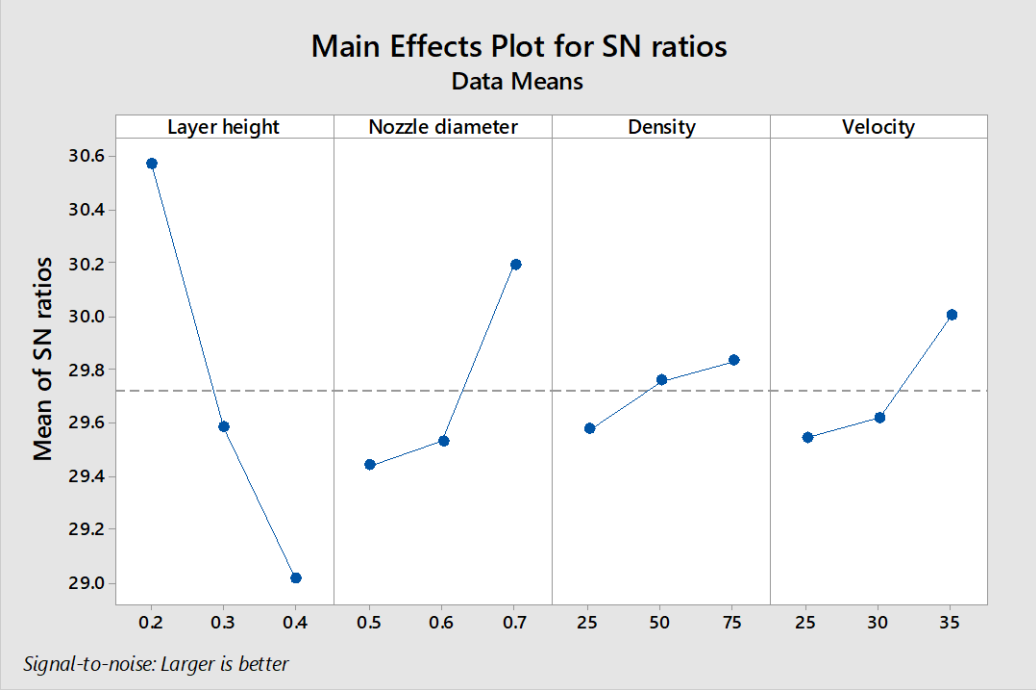

Figure 33: Main plot for S/N ratio, Elastic limit

As mentioned before, to validate the results, (Fig. 34) must be taken into account. In Elastic limit case, the residual plot for means shows a histogram with the desired bell shape and the different point aligned in the normal probability plot. As well, fits show a random distribution of points.

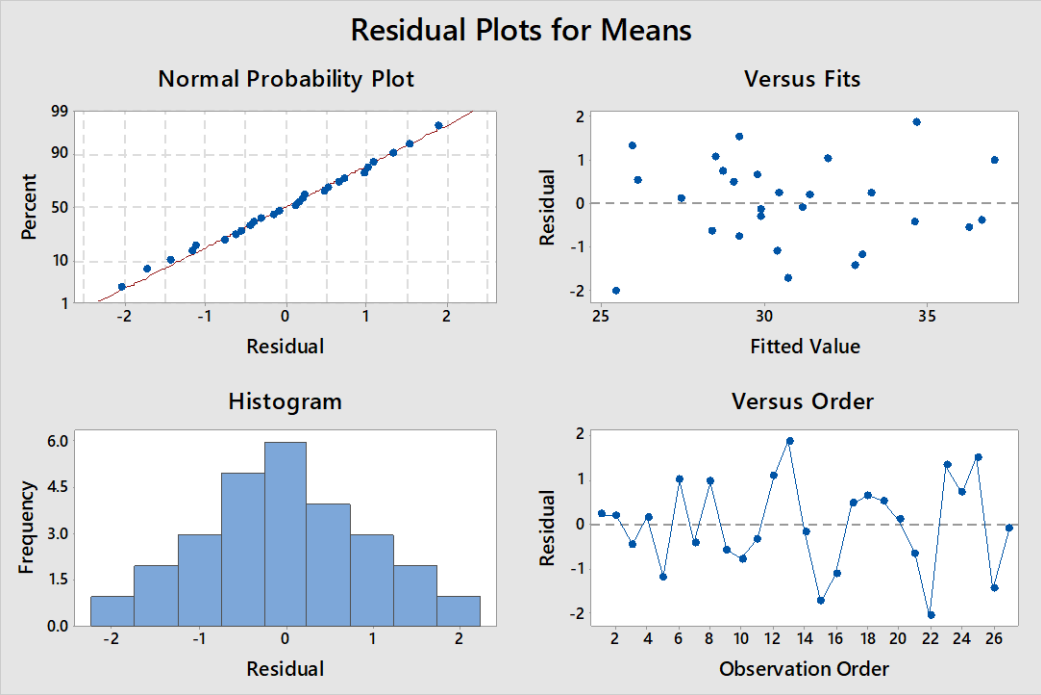

Figure 34: Residual plot for means, Elastic limit

6.3. Maximum tension (σ_{max})

First of all, it is necessary to look at the significance of the different factors on this property, it is followed by a 5% significance level (α = 0.05) shown in (Table. 10).

Table 10: p-values of means, Maximum tension

Factor	P-value
Layer height	0.000
Nozzle diameter	0.001
Density	0.007
Printing velocity	0.869

Based on the obtained p-values from the factors, it can be mention a notable significance of layer height, nozzle diameter, and infill density on the maximum tension. Following, we can found the best level of these factors in (Fig. 35).

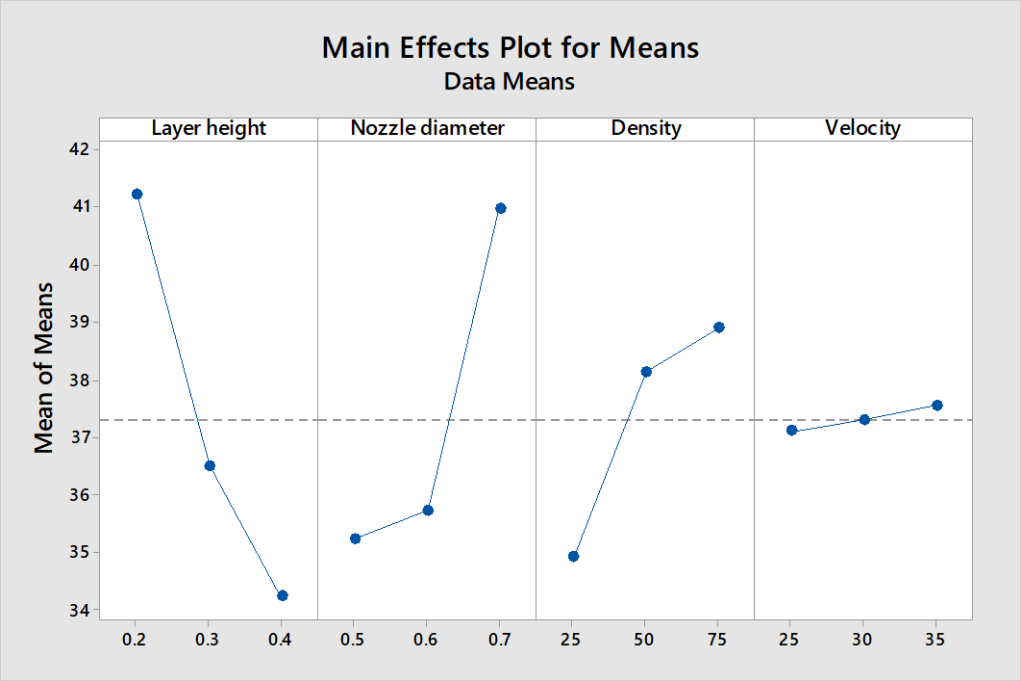

Figure 35: Main effects plot for means, Maximum tension

In order to the selected variations of the factors in this project, the best level of the layer height, nozzle diameter, and infill density to be influent on the maximum tension are 0.2 mm, 0.7 mm, and 75 % respectively.

The interaction plot of means (Fig. 36) shows that could be an interaction between Nozzle diameter and Layer height.

Figure 36: Interaction plot for means, Maximum tension

On the other hand, (Table. 11) shows that the p-value is higher than 0.05, therefore the interaction between parameters should not be taken into account.

Table 11: p-value interaction of means, Maximum tension

Factor	P-value
Layer height *Nozzle diameter	0.131
Layer height * Density	0.319
Nozzle diameter *Density	0.489

The SN relationship (signal to noise) is the value of the output signal of each parameter and the noise or error of this model. It must be taken into account to validate the robustness of the test performed. To determine the robustness of each factor in the face of possible external variability, the p-value is checked by establishing a 5% significance level ($\alpha = 0.05$) (Table. 12).

Table 12: p-values of S/N, Maximum tension

Factor	P-value
Layer height	0.001
Nozzle diameter	0.002
Density	0.008
Printing velocity	0.864

The notably influential parameters for the S/N of the maximum tension are layer height, nozzle diameter, and density which the level of theses factor can be found in (Fig. 37). The lower height of layer can result the higher maximum tension which is 0.2 mm. The bigger nozzle diameter (0.7 mm) and higher percentage of density (75 %) give bigger maximum tension. Printing velocity does not make any sensitive effect on this property.

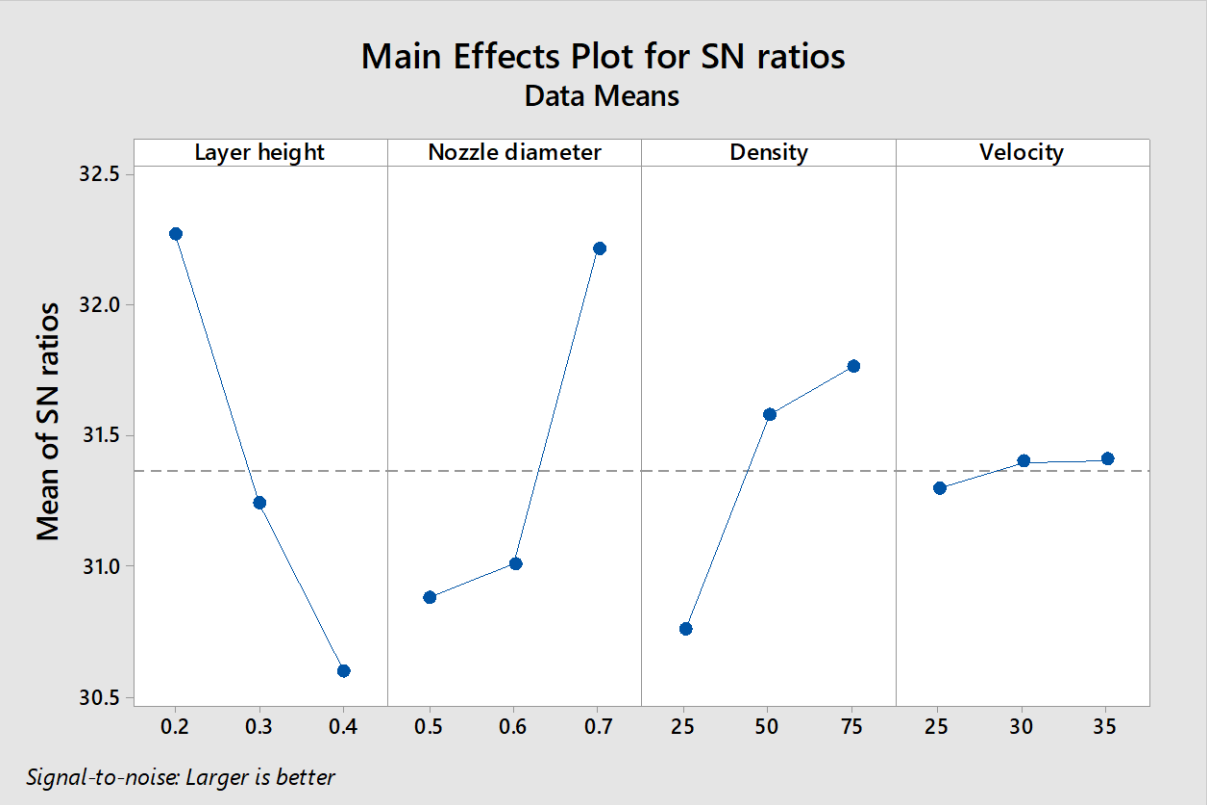

Figure 37: Main effect plot for S/N ratio, Maximum tension

In (Fig. 38) can be seen the residual plots for means for maximum tension. In contrast with the previous section, the residual plot for maximum tension does not show a normal distribution. The histogram is displaced, and the points of normal probability plot are not completely aligned.

However, the fits graphs shows a random distribution which means that there is not an accumulation of errors alongside the test.

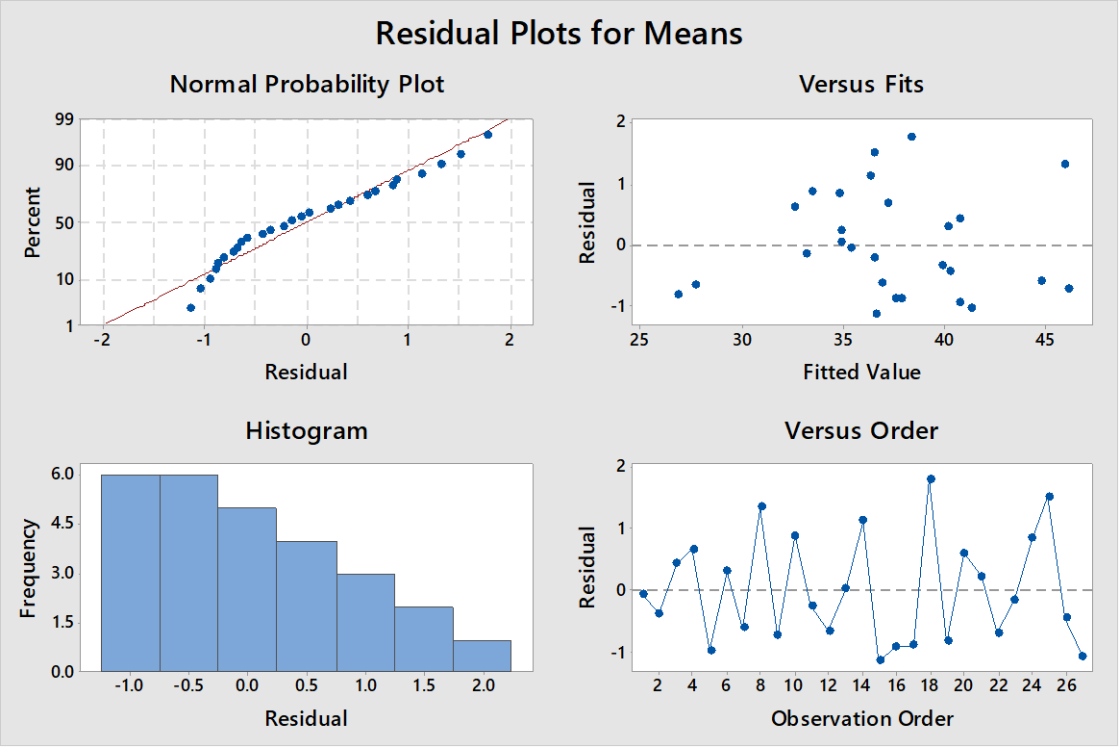

Figure 38: Residual plot for means, Maximum tension

6.4. Maximum elongation

First of all, take into account the influence of the different factors on this property, it is followed by a 5% significance level (α = 0.05) shown in (Table. 13).

Table 13: p-values of means, Maximum elongation

Factor	P-value
Layer height	0.310
Nozzle diameter	0.004
Density	0.003
Printing velocity	0.293

In this case, the layer height is not an influential parameter whereas infill density and nozzle diameter have shown significances p-value on the maximum elongation. In (Fig. 39) we can found the best level of these factors.

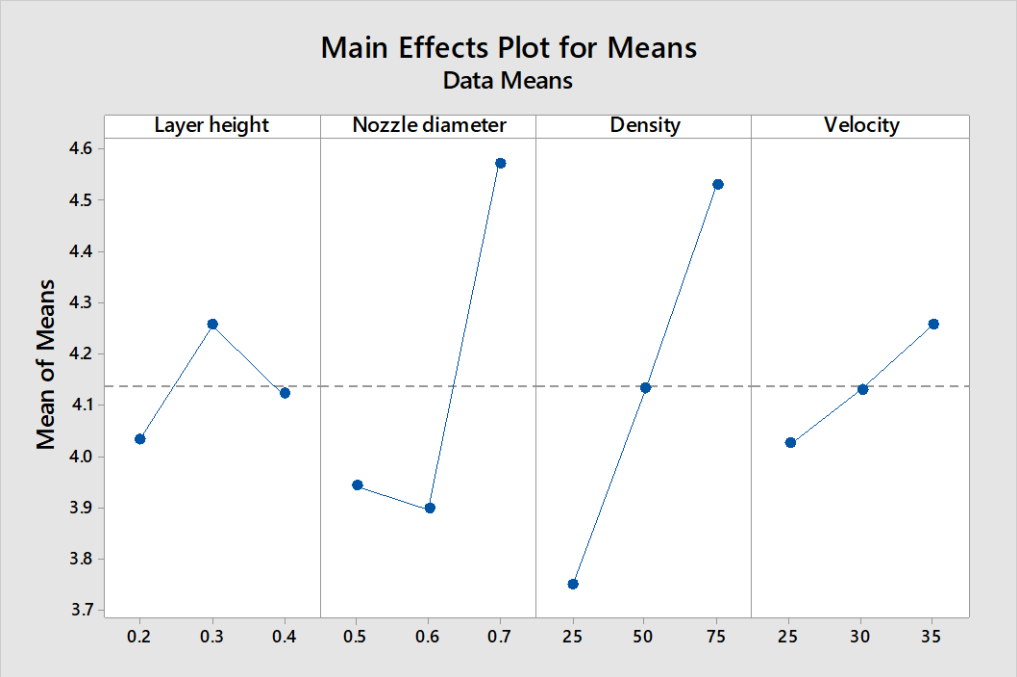

Figure 39: Main effects plot for means, Maximum elongation

In order to the selected variations of the factors in this project, the best level of the infill density and nozzle diameter to influence on the maximum elongation are 75 % and 0.7 mm respectively.

As it can be seen in (Fig. 40) could be different infarctions between the parameters and levels. As mentioned before, to consider influential the interaction of parameters we have to take a look to the p-value.

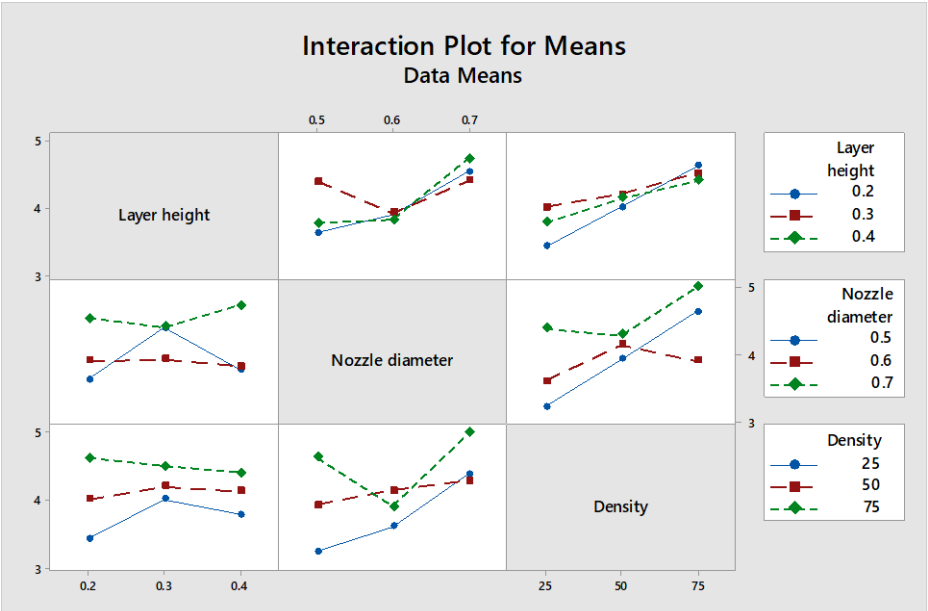

Figure 40: Interaction plot for means, Maximum elongation

In this case, the p-value for the interaction between Nozzle diameter and Density is lower than 0.05. It means the interaction between these parameters is significant. It also means that the interaction between the levels of this both parameters can affect on the maximum elongation value.

Table 14: p-value interaction of means, Maximum elongation

Factor	P-value
Layer height *Nozzle diameter	0.107
Layer height * Density	0.345
Nozzle diameter *Density	0.040

The SN relationship (signal to noise) is the value of the output signal of each parameter and the noise or error of this model. It must be taken into account to validate the robustness of the test done. To determine the robustness of each factor in the face of possible external variability, the p-value is checked by establishing a 5% significance level ($\alpha = 0.05$) (Table. 15).

Table 15: p-values of S/N, Maximum elongation

Factor	P-value
Layer height	0.160
Nozzle diameter	0.002
Density	0.002
Printing velocity	0.204

The notably influential parameters for the S/N of the maximum elongation are nozzle diameter, and density which the level of theses factor can be found in (Fig. 41). The bigger diameter of nozzle can result the higher maximum elongation which is 0.7 mm and higher percentage of density (75 %) give bigger maximum elongation. Printing velocity and layer height do not make any sensitive effect on this property.

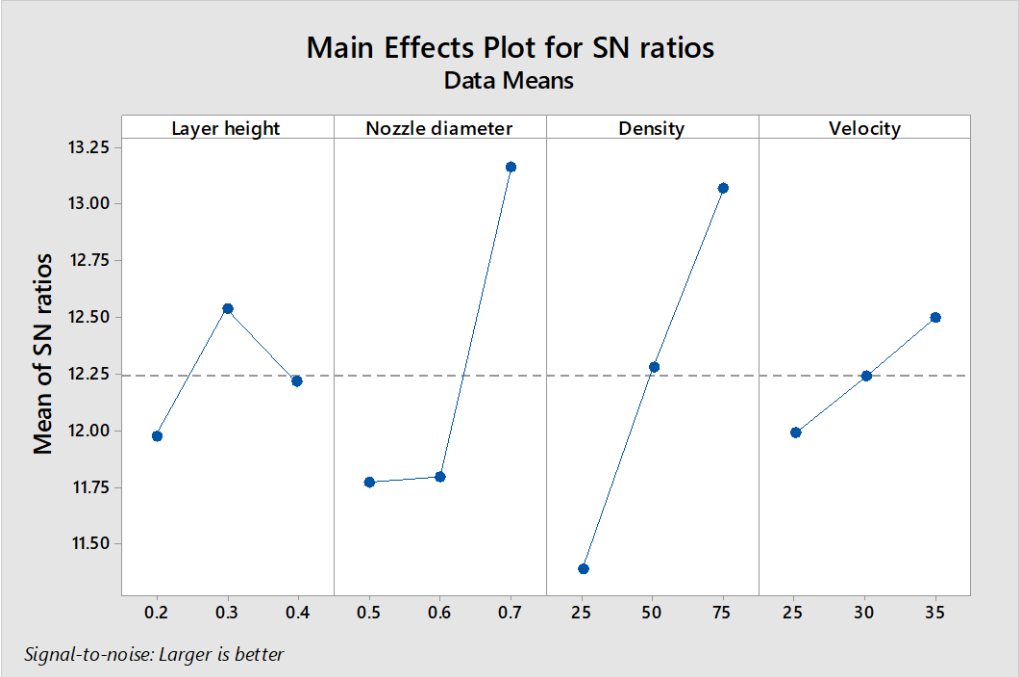

Figure 41: Main effect plot for S/N ratio, Maximum elongation

Residual plots of means for maximum elongation show a quite normal distribution. As can be seen in (Fig. 42), the points are aligned with the normal probability plot. The histogram also shows a normal distribution, but a bit displaced. As in the previous case, fits shows a cloud of random distribution of points.

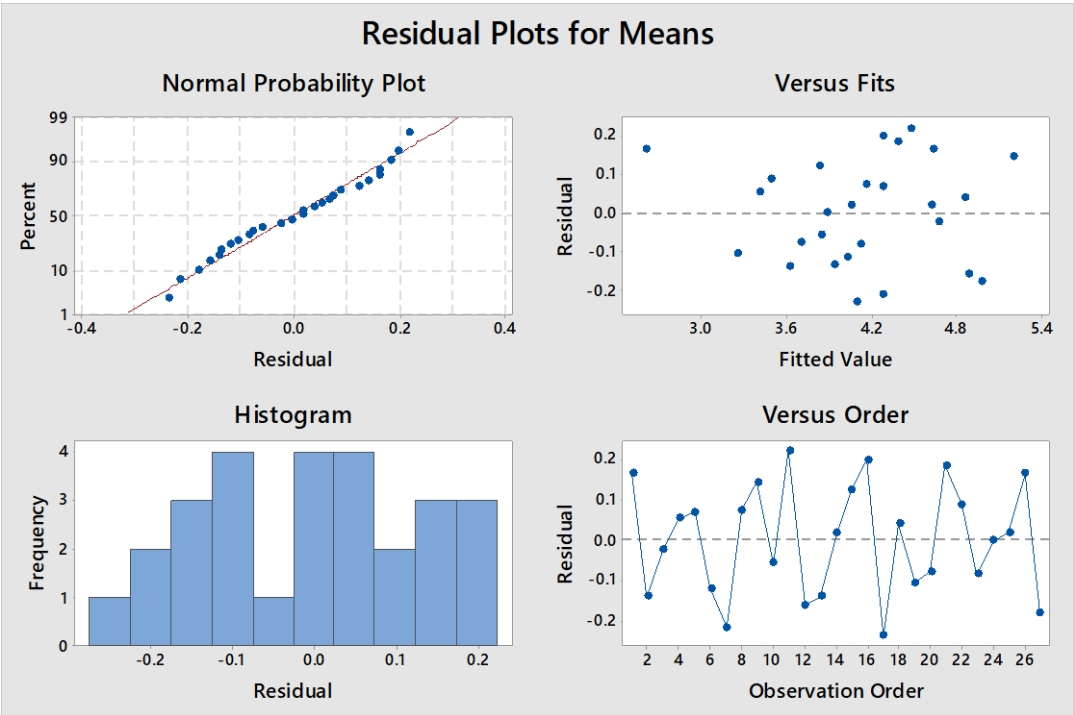

Figure 42: Residual plot for means, Maximum elongation

7. Results discussion

An overview of the results is summarized in (Table. 16). First of all the most influential parameters on the responses are shown in green, the yellow cells illustrate the threshold factors, and not significant ones are in red based on p-values. In the other side, the best selected level of each parameter is indicated in the cells.

Table 16: Abstract of results and significance

Factor	Responses			
	Elastic characteristics		Plastic characteristics	
	Young Modul (E)	Elastic Limit ($Rp_{0,2}$)	Maximum Tension (σ_{max})	Maximum elongation (ε)
Layer Height (mm)	0.2	0.2	0.2	0.3
Nozzle Diameter (mm)	0.7	0.7	0.7	0.7
Fill Density (%)	50	75	75	75
Printing Velocity (mm/s)	35	35	35	35

In (Table. 17) the set of parameters to optimize rigidity and flexural resistance within the range of the experiment are illustrated. The criterion will be followed in order to define the best parameters:

- The level of parameter that achieve the high response.
- In case of different value of level in the same parameter, the chosen level must be the one which has the less p-value.

Table 17: Optimized level of parameters

Factor	Chosen level
Layer height (mm)	0.2
Nozzle diameter (mm)	0.7
Density (%)	75
Printing velocity (mm/s)	35

Below the significances of each parameter are explained generally on the related responses studied within this project.

7.1. Layer height

This parameter results more important effect on the responses (except for maximum elongation). In order to the main effects of means plot it can be seen that, the lower layer height (0.2 mm) maximizes the values of responses.

It means the lower height of layer causes more cohesive interaction between the layers, fulfill the gaps, and more solidity consequently.

7.2. Nozzle diameter

As already mentioned, in all cases the response has been maximized with the bigger diameter of the extruder (0.7 mm) since it allows to deposit more material during the fabrication so, the stronger welding between fibers occurs achieving more rigid samples. This rigidity of the material makes the samples more difficult to bend withstand higher tension.

Because of that, this parameter is the most influential on maximum tensions and maximum elongation based on the plots and the p-values are shown in previous section.

7.3. Infill density

Fill density is shown as a non-significant parameter on the Young's modulus and elastic limit. However it has influence on the other two properties, since it affects on the solidity percentage of inside the specimens. In the other hand, regarding to the means effects plots the higher percentages gives more values for each required responses.

7.4. Printing velocity

Printing velocity is the lowest influential parameter on the responses. It is caused because of the small size of the samples. This size does not allow the material to be cold before the following layer, therefore all of the layer are well-melded between them. If the size of the samples will be bigger, as a hypothesis, the melded material between layers would be determined by the printing velocity.

As well as, the printing velocity is a very restricted parameter in FFF due to the mentioned above, so different levels of printing speed must be in the ratio between 25 and 35 mm/s.

8. Comparison between PLA/Timberfill

Finally, it is interesting to compare the results achieved in this project done on Timberfil material with another most common used material PLA, since Timberfill is a composite of PLA and wood fibres.

(PLA) is a polymer made up of polylactic acid molecules with properties resemble to polyethylene, it is obtained mainly from organic matter. It has a relatively low resistance but a higher hardness than high thermoplastic similar.

The used data to carry out the comparison are obtained from Oriol Traver's project [6] which has been done in the same condition of current work in this research group. (Table. 18) shows the best combination set of parameters obtained for PLA and Timberfill material.

Table 18: PLA levels of best combination

	Chosen level	
Factor	PLA	Timberfill
Layer height (mm)	0.1	0.2
Nozzle diameter (mm)	0.6	0.7
Density (%)	75	75
Printing velocity (mm/s)	20	35

Considering the selected values for each parameter in that project, it can be seen how practically the same factors have been found as a recommendation in the present work on the Timberfill. In PLA case, Layer height 0.1 mm was selected as the lowest. Nozzle diameter and density were chosen as the highest. For Timberfill, is the same case the lowest Layer height; and the higher nozzle diameter and Infill density.

In spite of printing velocity that is revers with the Timberfill results. It means for PLA lower speed causes higher flexural resistance. Also it has shown more significant on the results.

On the other hand, it is necessary to compare the maximum values of each mechanical properties achieved by both projects. These comparisons are indicated in (Table. 19).

Table 19: Maximum values achieved for PLA/Timberfill

Maximum values		
Factor	**Timberfill**	**PLA**
Young's Modulus (GPa)	2.41	3.70
Elastic Limit (Mpa)	38.06	90.8
Maximum Tension (Mpa)	47.26	109.5
Maximum Elongation (%)	5.34	6.21

As it can be seen form the table, the obtained results for PLA are higher in each mechanical property.

This mechanical behavior is due to Timberfill is a composite of wood fibers and a matrix of PLA, whereas PLA is a polymer. The wood fibers create discontinuities in the matrix causing lower ductility in Timberfill than PLA.

The wood fibers act as a nail transferring the load to PLA matrix alongside the fibers and the breakage advance is forced to pass through the nails which are perpendicular to the tension. It concentrates the tension on the PLA matrix and decreases the mechanical resistance to bend.

9. Conclusion

To sum up, the following conclusions have been obtained based on the results.

This project shows the effects of different combination of parameters on the mechanical properties. The selected parameters are: Layer height, Nozzle diameter, Infill density and printing velocity. Infill pattern and orientation reminded constant. The mechanical behaviors to be optimized are: Young modulus, Elastic limit, Maximum tension and Maximum Elongation.

The best combination of parameters which allows optimizing flexural properties is:

- Layer height: 0.2 mm
- Nozzle diameter: 0.7 mm.
- Infill density: 75%
- Printing velocity: 35 mm/s.

Regarding to the influence of each parameter on the results:

- The most influential parameter is the Layer height, followed by Nozzle diameter. Both are so effective on the results but did not show a significant interaction between them.
- Printing velocity has no significant effects on the results, based on the p-value achieved for each studied mechanical property.
- The interaction between nozzle diameter and Infill density is significant in maximum elongation. The combination of the different levels of these parameters directly affects on the value of the maximum elongation.
- The significant parameters are selected. However, the criteria for the no influential parameters can be based on the time needed to manufacture, avoid waste huge amount of material or choose it according to the pricing of the process. In this case, only Printing velocity has been no significant, however the level which can achieve the optimal mechanical properties is the highest one. It means, the time to manufacture a sample is the quickest.

Budget

In this section, the cost of the project is detailed. This cost has been divided in 3 different sections:

- Material cost
- Human resources
- Electricity cost

It must be taken into account that the laptop, 3D printer, metrology devices and test machines are not showed in this budget because there were not necessary to buy or pay a rent for them.

(Table 20) shows the cost of each tested sample. The cost has been calculated using the weight of each sample and the price per gram of Timberfill. The last line is the cost of the previous samples printed to test and calibrate the test machine.

Table 20: Cost of Timberfill

Sample	Sample weight (gr)	Timberfill (€/gr)	Total €
1.1	2.849	0.059	0.17
1.2	2.841	0.059	0.17
1.3	2.811	0.059	0.17
1.4	2.861	0.059	0.17
1.5	2.849	0.059	0.17
2.1	3.016	0.059	0.18
2.2	3.085	0.059	0.18
2.3	3.041	0.059	0.18
2.4	2.972	0.059	0.18
2.5	3.014	0.059	0.18
3.1	3.136	0.059	0.19
3.2	3.195	0.059	0.19
3.3	3.164	0.059	0.19
3.4	3.152	0.059	0.19
3.5	3.141	0.059	0.19
4.1	2.889	0.059	0.17
4.2	2.843	0.059	0.17
4.3	2.913	0.059	0.17
4.4	2.904	0.059	0.17
4.5	2.905	0.059	0.17
5.1	3.254	0.059	0.19
5.2	3.004	0.059	0.18
5.3	3.016	0.059	0.18
5.4	3.131	0.059	0.18

5.5	2.954	0.059	0.17
6.1	3.296	0.059	0.19
6.2	3.247	0.059	0.19
6.3	3.294	0.059	0.19
6.4	3.236	0.059	0.19
6.5	3.248	0.059	0.19
7.1	3.072	0.059	0.18
7.2	3.144	0.059	0.19
7.3	3.111	0.059	0.18
7.4	3.091	0.059	0.18
7.5	3.132	0.059	0.18
8.1	3.262	0.059	0.19
8.2	3.238	0.059	0.19
8.3	3.251	0.059	0.19
8.4	3.124	0.059	0.18
8.5	3.156	0.059	0.19
9.1	3.377	0.059	0.20
9.2	3.343	0.059	0.20
9.3	3.397	0.059	0.20
9.4	3.421	0.059	0.20
9.5	3.395	0.059	0.20
10.1	2.693	0.059	0.16
10.2	2.832	0.059	0.17
10.3	2.841	0.059	0.17
10.4	2.735	0.059	0.16
10.5	2.746	0.059	0.16
11.1	2.886	0.059	0.17
11.2	2.882	0.059	0.17
11.3	2.874	0.059	0.17
11.4	2.903	0.059	0.17
11.5	2.908	0.059	0.17
12.1	3.112	0.059	0.18
12.2	3.215	0.059	0.19
12.3	3.109	0.059	0.18
12.4	3.126	0.059	0.18
12.5	3.101	0.059	0.18
13.1	3.003	0.059	0.18
13.2	3.092	0.059	0.18
13.3	3.016	0.059	0.18
13.4	3.108	0.059	0.18
13.5	3.111	0.059	0.18
14.1	3.356	0.059	0.20

14.2	3.353	0.059	0.20
14.3	3.217	0.059	0.19
14.4	3.211	0.059	0.19
14.5	3.141	0.059	0.19
15.1	2.747	0.059	0.16
15.2	3.129	0.059	0.18
15.3	3.227	0.059	0.19
15.4	3.209	0.059	0.19
15.5	3.443	0.059	0.20
16.1	2.826	0.059	0.17
16.2	2.687	0.059	0.16
16.3	3.054	0.059	0.18
16.4	2.744	0.059	0.16
16.5	3.003	0.059	0.18
17.1	3.169	0.059	0.19
17.2	3.302	0.059	0.19
17.3	3.237	0.059	0.19
17.4	3.045	0.059	0.18
17.5	3.307	0.059	0.20
18.1	3.466	0.059	0.20
18.2	3.473	0.059	0.20
18.3	3.474	0.059	0.20
18.4	3.456	0.059	0.20
18.5	3.468	0.059	0.20
19.1	2.394	0.059	0.14
19.2	2.788	0.059	0.16
19.3	2.949	0.059	0.17
19.4	2.817	0.059	0.17
19.5	2.329	0.059	0.14
20.1	2.833	0.059	0.17
20.2	2.858	0.059	0.17
20.3	2.85	0.059	0.17
20.4	2.847	0.059	0.17
20.5	2.885	0.059	0.17
21.1	3.359	0.059	0.20
21.2	3.348	0.059	0.20
21.3	2.975	0.059	0.18
21.4	2.969	0.059	0.18
21.5	2.882	0.059	0.17
22.1	3.037	0.059	0.18
22.2	3.036	0.059	0.18
22.3	2.924	0.059	0.17

22.4	3.081	0.059	0.18
22.5	3.063	0.059	0.18
23.1	3.36	0.059	0.20
23.2	3.355	0.059	0.20
23.3	3.404	0.059	0.20
23.4	3.315	0.059	0.20
23.5	3.309	0.059	0.20
24.1	3.392	0.059	0.20
24.2	3.374	0.059	0.20
24.3	3.371	0.059	0.20
24.4	3.323	0.059	0.20
24.5	3.399	0.059	0.20
25.1	3.082	0.059	0.18
25.2	3.09	0.059	0.18
25.3	3.073	0.059	0.18
25.4	2.673	0.059	0.16
25.5	3.067	0.059	0.18
26.1	3.146	0.059	0.19
26.2	3.257	0.059	0.19
26.3	3.101	0.059	0.18
26.4	3.143	0.059	0.19
26.5	3.136	0.059	0.19
27.1	3.508	0.059	0.21
27.2	3.38	0.059	0.20
27.3	3.483	0.059	0.21
27.4	3.162	0.059	0.19
27.5	3.462	0.059	0.20
Previous samples to test	32.24	0.059	1.91
		Total Cost	**26.59**

The consumable equipment is shown in (Table 21).

Table 21: Consumible equipment

Concept	Qty.	Unit cost (€)	Total cost (€)
Timberfill	1	26.59	26.59
Nozzle diameter 0.5	1	9.68	9.68
Nozzle diameter 0.6	1	9.68	9.68
Nozzle diameter 0.7	1	9.68	9.68
3DLAC 400 ml	1	7.50	7.50
Small material	1	12.00	12.00
		Total Cost	**75.13**

Electricity costs in Spain is 0.12 €/kWh. In (Table 22) can be seen the cost of the energy consumed by the devices used to carry out this project.

Table 22: Energy cost

Concept	Hours	kWh/h	€/kWh	Total cost (€)
Pyramid 3D	101.25	0.55	0.12	6.68
HP Intel Core i5 (laptop)	374	0.44	0.12	19.61
Flexural test machine	4.5	0.76	0.12	0.41
Camera + flash	4.5	0.25	0.12	0.14
Spider data recorder	4.5	0.31	0.12	0.17
		Total Cost		**27.01**

Finally, it has been established a cost of 20 €/h for human resources. In the table below (Table 23) can be seen the costs of the hours dedicated to this project.

Table 23: Human resources cost

Concept	Hours	Cost/h	Total cost (€)
Documentation and state of art	24	20	480.00
Experimental design	80	20	1,600.00
Print the samples	101.25	20	2,025.00
Experimental test	4.5	20	90.00
Analysis of results	270	20	5,400.00
		Total Cost	**9,595.00**

To summarize, (Table 24) gives the total amount of the project.

Table 24: Summary cost

Concept		Total cost (€)
Consumable equipment		75.13
Energy cost		27.01
Human resources		9,595.00
	Total Cost	**9,697.14**

The total cost of the project is **9,697.14 €.**

Bibliography

1. Optfain E., *Análisis cualitativo del impacto de la Impresión 3D en la industria y la economía*. Informe cero. 1.

2. EP., *Crean células madre con impresoras 3D y abren el camino a la "fabricación" de órganos*. 20minutos.es, 2013 february 08. Available from: https://www.20minutos.es/noticia/1725004/0/celulas-madre/impresoras-3d/fabricar-organos/#xtor=AD-15&xts=467263

3. Travieso-Rodriguez JA., *Impressió 3D.* Universitat Politècnica de Catalunya 2017.

4. Additive Manufacturing Research Group | Loughborough University. Available from: http://www.lboro.ac.uk/research/amrg/about/whatisam/

5. Gomez-Gras, G., et al., Fatigue performance of fused filament fabrication PLA specimens. Materials & Design, 2018. 140: p. 278-285.

6. Traver, O., *Estudio de la influencia del proceso de fabricación en las propiedades mecánicas de especímenes moldeados por deposición fundida.* Universitat Politecnica de Catalunya 2018.

7. Adrover Montserrat, B., *Estudi de les propietats mecàniques de peces fabricades per impressió 3D*. Universitat Politècnica de Catalunya 2018.

8. Gurrala PK, Regalla SP., *Part strength evolution with bonding between filaments in fused deposition modelling*. Virtual Phys Prototyp. Taylor & Francis; 2014. **39**(6): p. 933-961.

9. Tymrak, B.M., M. Kreiger, and J.M. Pearce*, Mechanical properties of components fabricated with open-source 3-D printers under realistic environmental conditions*. Materials & Design, 2014. 58: p. 242-246.

10. Jerez Mesa, R., et al. *Comparison of thermal performance of 3D printer liquefiers through finite element models. in Proceeding of 20th International Research/Expert Conference"* Trends in the Development of Machinery and Associated Technology" TMT 2016. 2016.

11. 3D Printing; Simplify3D. Available from: https://www.simplify3d.com/support/

12. Slic3r Manual, *Infill Patterns and Density*. Available from: http://manual.slic3r.org/expert-mode/infill.

13. Puigoriol-Forcada, J. M., Alsina, A., Salazar-Martín, A. G., Gomez-Gras, G., & Pérez, M. A. *Flexural Fatigue Properties of Polycarbonate Fused-deposition Modelling Specimens.* Materials & Design. 2018.

14. Balderrama-Armendariz, C.O., et al., *Torsion analysis of the anisotropic behavior of FDM technology.* The International Journal of Advanced Manufacturing Technology, 2018: p. 1-11.

15. Cantrell, J.T., et al*., Experimental characterization of the mechanical properties of 3D-printed ABS and polycarbonate parts*. Rapid Prototyping Journal, 2017. 23(4): p. 811-824.

16. Afrose, M.F., et al*., Effects of part build orientations on fatigue behaviour of FDM-processed PLA material.* Progress in Additive Manufacturing, 2015. 1(1-2): p. 21-28.

17. Shabat, D., et al., *Mechanical and structural characteristics of fused deposition modeling ABS material*. Annals of "Dunarea de Jos" University, Fascicle XII, Welding Equipment and Technology, 2017. 28: p. 16-24.

18. Croccolo, D., M. De Agostinis, and G. Olmi, *Experimental characterization and analytical modelling of the mechanical behaviour of fused deposition processed parts made of ABS-M30.* Computational Materials Science, 2013. 79: p. 506-518.

19. Arivazhagan, A. and S. Masood, *Dynamic mechanical properties of ABS material processed by fused deposition modelling*. Int. J. Eng. Res. Appl, 2012. 2(3): p. 2009-2014.

20. Fu, S.-Y., et al., *Effects of particle size, particle/matrix interface adhesion and particle loading on mechanical properties of particulate–polymer composites*. Composites Part B: Engineering, 2008. 39(6): p. 933-961.

21. Timberfill Champagne; Fillamentum. Available from: https://fillamentum.com/collections/timberfill/products/timberfill-champagne?variant=1261597627

22. Casadesus, O., *Estudi de propietats mecàniques de l'Acrilonitril-Butadiè-Estirè per a impressió tri-dimensional per Fused Filament Fabrication*. Universitat Politecnica de Catalunya 2018.

23. ASTM international., *Standard Test Method for Flexural Properties of Unreinforced and Reinforced Plastics and Electrical Insulating Materials by Four-Point Bending.* Published June 2002.

24. Pilipović, A., P. Raos, and M. Šercer, *Experimental analysis of properties of materials for rapid prototyping.* The International Journal of Advanced Manufacturing Technology, 2007. 40(1-2): p. 105-115.

25. Es-Said, O.S., et al*., Effect of Layer Orientation on Mechanical Properties of Rapid Prototyped Samples*. Materials and Manufacturing Processes, 2000. 15(1): p. 107-122.

26. Ning, F., et al*., Additive manufacturing of carbon fiber-reinforced plastic composites using fused deposition modeling: Effects of process parameters on tensile properties*. Journal of Composite Materials, 2017. 51(4): p. 451-462.

27. Bassett, K., R. Carriveau, and D.S.K. Ting, *3D printed wind turbines part 1: Design considerations and rapid manufacture potential*. Sustainable Energy Technologies and Assessments, 2015. 11: p. 186-193.

28. Wittbrodt, B. and J.M. Pearce, *The effects of PLA color on material properties of 3-D printed components*. Additive Manufacturing, 2015. 8: p. 110-116.

29. Bellini, A. and S. Güçeri, *Mechanical characterization of parts fabricated using fused deposition modeling*. Rapid Prototyping Journal, 2003. 9(4): p. 252-264.

30. Casavola, C., et al., *Orthotropic mechanical properties of fused deposition modelling parts described by classical laminate theory*. Materials & Design, 2016. 90: p. 453-458.

31. Domingo-Espin, M., et al., *Mechanical property characterization and simulation of fused deposition modeling Polycarbonate parts*. Materials & Design, 2015. 83: p. 670-677.